JAAS

Journal of Analytical Atomic Spectrometry

238 Pu

239 Pu

240 Pu

241 Pu

242 Pu

244 Pu
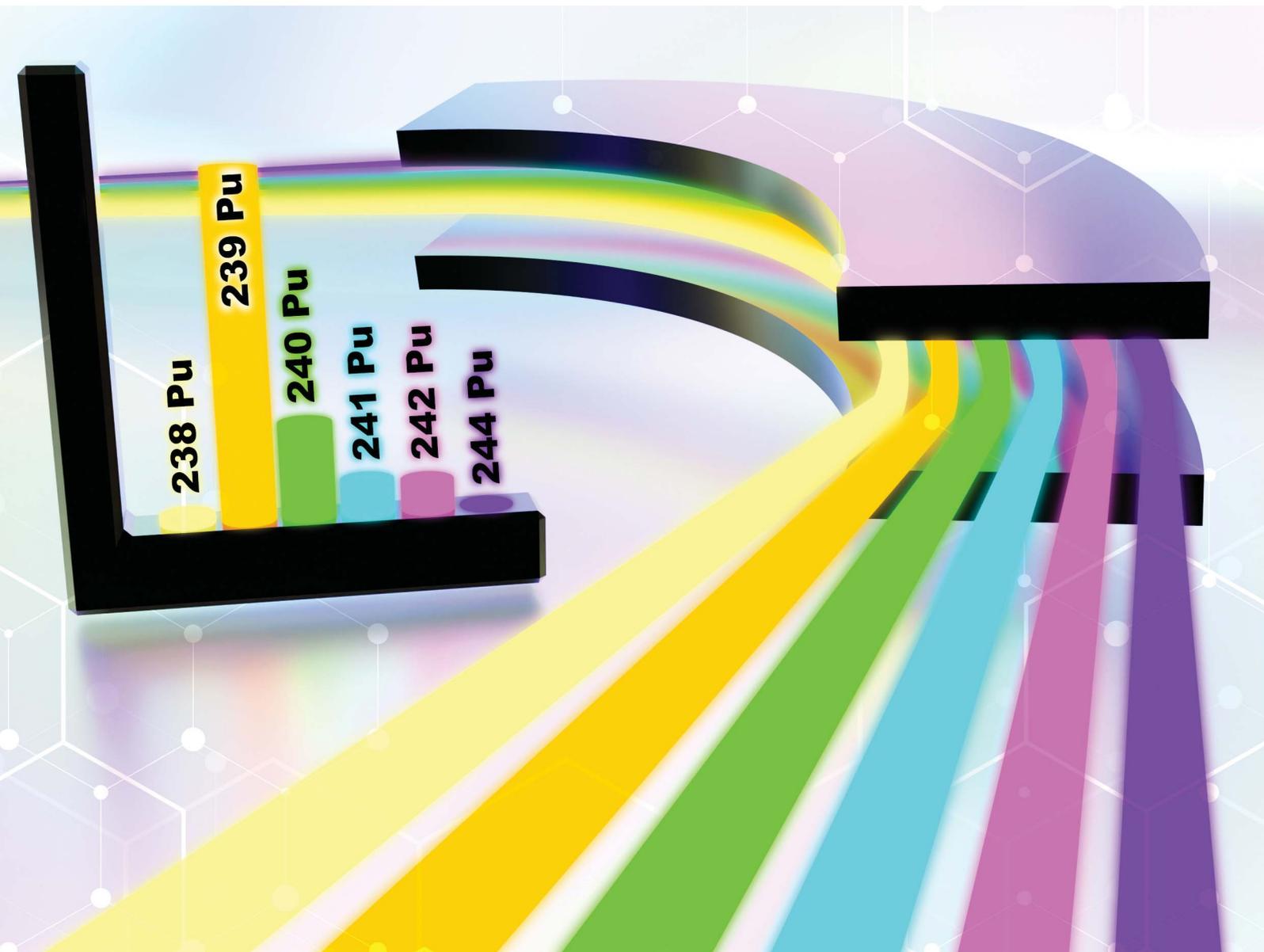
CRITICAL REVIEW

Kattathu Joseph Mathew

Plutonium isotope ratio measurements by total evaporation-thermal ionization mass spectrometry (TE-TIMS): an evaluation of uncertainties using traceable standards from the New Brunswick Laboratory

ROYAL SOCIETY OF CHEMISTRY

CRITICAL REVIEW

Check for updates

Plutonium isotope ratio measurements by total evaporation-thermal ionization mass spectrometry (TE-TIMS): an evaluation of uncertainties using traceable standards from the New Brunswick Laboratory†

Kattathu Joseph Mathew [iD] ‡

The accuracy and precision of isotope amount ratio measurements using thermal ionization mass spectrometry (TIMS) instrumentation are described, and the measurement of Pu materials is emphasized. The mass fractionation observed for Am, Ga, Pu, and U for isotope amount ratio measurements using the total evaporation (TE) technique is compared with theoretical estimates to demonstrate the advantage of the TE methodology and to investigate systematic biases in the major isotope amount ratios of U and Pu certified reference material (CRM) standards from the U.S. provider of CRMs. The quality of the Pu isotopic data generated by TIMS instruments in an analytical laboratory is demonstrated by the application of the double ratio technique to estimate the ^{241}Pu half-life. Analytical data on traceable Pu CRMs from the New Brunswick Laboratory (NBL), generated as part of routine measurements supporting various programs, are used for this half-life estimation. Although the ^{241}Pu abundances in CRMs of 136, 137, 138, and 126-A are approximately 200–2000× smaller than those in the ^{241}Pu material used in the previous Institute for Reference Materials and Measurements (IRMM) evaluation of the ^{241}Pu half-life, the half-life value estimated in this work shows excellent agreement with the currently accepted value from the IRMM. This agreement also demonstrates the pedigree of the Pu isotopic standards from the NBL and the quality of the isotope amount ratio measurements using TIMS instrumentation. For both the major and minor Pu isotope amount ratios, this report describes the relative importance of the factors affecting the uncertainty of TIMS measurements, which are considered the gold standard in isotope ratio measurements (LA-UR-24-29199).

Introduction

For the third consecutive year, the International Atomic Energy Agency (IAEA) has revised its forecast for the worldwide growth of nuclear energy.[1] These revisions demonstrate greater adoption of nuclear technologies to meet energy needs associated with economic growth, and national efforts towards energy independence and diversification of energy sources, especially in emerging fields, such as artificial intelligence. The prevalence of nuclear technologies creates unique challenges for the nuclear safeguards and nonproliferation communities, which implement measures to prevent the diversion of nuclear

materials for clandestine activities. The IAEA has taken a leadership role in setting up the framework for the safeguarding of nuclear materials and has established procedures to provide credible assurance to the international community that nuclear materials subject to safeguards are not diverted from their declared peaceful uses.[2–5] The nuclear forensic community has developed innovative analytical techniques to address the proliferation challenges associated with interdicted special nuclear materials (SNMs)[6–23] and to ensure that the history of materials is consistent with their declared uses. IAEA data indicate that although the materials most likely to be used in a clandestine nuclear explosive device are highly enriched fissile materials, U materials commonly intercepted in illicit trafficking incidents have close to natural or low enrichment of the fissile ^{235}U isotope.[24–28] These less "attractive" materials (from early processes like mining and milling of the nuclear fuel cycle) are more susceptible to theft/diversion because of the less restrictive security arrangements associated with these processes than those associated with securely guarded highly enriched materials that can be readily used in clandestine

Material Signatures & Isotopic Standards Group, Chemical Sciences Division, Oak Ridge National Laboratory, 1 Bethel Valley Road, Oak Ridge, TN 37831, USA. E-mail: mathewkj@ornl.gov

† Electronic supplementary information (ESI) available. See DOI: https://doi.org/10.1039/d5ja00140d

‡ Actinide Analytical Chemistry (C-AAC), Los Alamos National Laboratory, Los Alamos, NM 87545, USA.

This journal is © The Royal Society of Chemistry 2025

J. Anal. At. Spectrom., 2025, **40**, 1879–1901 | **1879**

activities. One compensatory measure instituted by the IAEA to counter the increased global nuclear proliferation threat is environmental sampling.[2,4,5] Environmental sampling is an effective mechanism for identifying undeclared nuclear activities involving U and Pu materials. The nuclear community has developed techniques to investigate individual U and Pu particles[29–34] collected during environmental sampling for forensic signatures. To unambiguously establish undeclared activities, multiple forensic signatures must demonstrate a consistent scenario about the production and process history of the SNM found to be out of regulatory control. The following is a partial list of attributes used to document the production history of SNMs:[6–23,35–43]

• Differences in the major element content and/or major isotope amount ratio.

• Differences in the elemental abundances of impurity elements.

• Small differences in the minor isotope amount ratios of the major elements.

• Chronometric ages.

• Concordance or discordance of the chronometric ages using different parent/daughter combinations.

Forensic analysis of SNMs is used to infer the intended use of the material and to understand its history, thereby enabling attribution of the source of the material. The chronometric dating of nuclear materials, whether they are intercepted (*e.g.*, stolen fuel pellets) or collected on purpose (*e.g.*, cotton swipes collected in operational nuclear facilities), is one of the most valuable techniques in nuclear forensic investigations.[44,45] When properly implemented, chronometric methodologies can simultaneously provide the material's "age" (*i.e.*, elapsed time since last purification of the decay products from the parent material), enrichment of the fissile isotope, actinide element concentrations, and minor isotope abundances. These characteristics are critical in establishing a material's source and processing history as well as identifying the potentially involved parties. Additionally, this information is crucial in evaluating the safeguards of SNMs and in verifying compliance with declared non-proliferation agreements by the countries involved.

Nuclear reactors produce Pu through neutron capture on ^{238}U. Neutron irradiation times and the conditions under which the reactor is operated dictate the relative abundances of the Pu isotopes produced. The Pu isotopic composition establishes the intended use of the Pu material. Weapons-grade, fuel-grade, and reactor-grade Pu contain approximately 4–7%, 7–19%, and >19% ^{240}Pu, respectively.[8,9,20–23] In addition to offering clues about intended use, the relative abundance of the Pu isotopic distribution may offer attribution information with respect to reactor type, operational characteristics, and the feed U material. The Pu assay results are a good indicator of intended use and of the general processing capability. The Pu element content (*i.e.*, assay) is a critical parameter for establishing an accurate age since separation of the Pu materials. The U and Pu contents in purified Pu materials change with time owing to radioactive decay of the Pu isotopes. The isotopes ^{234}U, ^{235}U, ^{236}U, and ^{238}U are produced by the α-decay of the isotopes ^{238}Pu,

^{239}Pu, ^{240}Pu, and ^{242}Pu, respectively. Quantification of the U daughter isotope and the abundances of the corresponding Pu parent isotope are essential for estimating the chronometric age of Pu materials.[13,15–18,20,43] Concordant ages from different Pu/U (parent/daughter) isotope pairs—$n(^{238}\text{Pu})/n(^{234}\text{U})$, $n(^{239}\text{Pu})/n(^{235}\text{U})$, $n(^{240}\text{Pu})/n(^{236}\text{U})$, and $n(^{242}\text{Pu})/n(^{238}\text{U})$—indicate that Pu was fully purified from U at some point in the material's history, and then U grew in without further addition of U from other sources.[17] Concordant ages from multiple Pu/U isotope combinations may also exclude the scenario where multiple Pu sources have been mixed to produce the material that is being scrutinized. Mixed sources can be the result of several factors, including processing, the starting materials being mixtures of isotopically distinct materials, unintentional contamination, or the blending of materials to alter the bulk isotopic compositions. In addition to constraining the time of purification or production of the nuclear material, chronometric ages can also establish or eliminate genetic links among different nuclear material samples. The $n(^{241}\text{Am})/n(^{241}\text{Pu})$ chronometer is another useful tool for elucidating the history of Pu materials. This chronometer often has uncertainties smaller than the corresponding U/Pu radiochronometric ages.[13,15–18,20,23,31,33,43] The larger uncertainties on the U/Pu chronometers, as compared with the Am/Pu age, are primarily due to the inability to correctly perform the tailing corrections in the minor isotope amount ratios of U because of the nonavailability of standards with isotopic abundances like the isotopic distribution of the progeny U and because of the uncertainties in the tailing corrections of the Pu minor isotope amount ratios.[46] The presence of ^{241}Am in a Pu material indicates that enough time has passed for the ^{241}Pu to have decayed to measurable quantities of ^{241}Am. The ^{241}Pu isotope has the shortest half-life (~14.3 years) among all Pu isotopes. The ^{241}Am concentration in a Pu material can provide information about the material's history. The decay relationship between ^{241}Pu and ^{241}Am produces an inherent chronometry pair for the determination of Pu age since separation. The $n(^{241}\text{Am})/n(^{241}\text{Pu})$ model ages calculated for a material would correspond to the production age of the material if the same assumptions stated earlier for Pu/U chronometry pairs are valid. Chemical processing of the Pu material that may have affected U and Am separations (from the Pu material) to varying degrees of completeness results in discordance between the U/Pu and Am/Pu chronometric ages. Chronometry principles have been successfully applied to elucidate the history of U materials, and multiple parent/daughter and parent/granddaughter chronometry pairs have been developed for the interrogation of U materials.[35–39,41–45] Recently, automated U/Pu separation techniques for environmental sample analysis have been developed,[47] enabling the chemical processes to catch up to the advances in the mass spectrometry instrumentation.

The U.S. Department of Energy's New Brunswick Laboratory (NBL; now called the NBL Program Office, or NBL PO) and the European Commission's Institute for Reference Materials and Measurements (IRMM; now called the Joint Research Center in Geel, or JRC-Geel) in Belgium are the major providers of certified reference material (CRM) standards for analytical

1880 | *J. Anal. At. Spectrom.*, 2025, **40**, 1879–1901

This journal is © The Royal Society of Chemistry 2025

measurements involving SNMs. Most of the U.S. supply of SNM standards was produced by the National Bureau of Standards (NBS) using thermal ionization mass spectrometry (TIMS) instrumentation and measurement techniques available from the 1950s to 1970s. In 1981, the responsibility for the production and certification of SNM standards was transferred from NBS to the NBL. NBS transferred their stock of standard reference materials (SRMs) to the NBL in 1987. The NBL renamed these standards as CRMs to differentiate them from the nonnuclear standards certified by the National Institute of Standards and Technology (NIST). Traceable standards provided by NBL PO and JRC-Geel include the following: U assay standards (available matrices include oxide, metal, solution, UF_6, and UF_4); U isotopic standards (available in oxide, metal, solution, and UF_6 matrices); a U trace impurity standard (only an oxide matrix is available); U ores (powder); gamma and neutron counting standards (encased U oxides); Pu assay standards (available matrices include oxide, metal, and nitrate); Pu isotopic standards (available matrices include oxide, metal, nitrate, and sulfate); a Th impurity standard (oxide); and Th ores (powder). The referenced literature[48–50] provides a documented, comprehensive history of IRMM and NBL CRMs. Standards needed for nuclear forensics investigations are different from those available from NBL PO and JRC-Geel.[51,52] For nuclear material control and accountability measurements a series of standards available from NBL PO and JRC-Geel are sufficient, though. The Pu isotopic standard CRMs 136, 137, and 138 are currently being recertified by NBL PO. See ESI S1† for the certified isotopic abundances and associated uncertainties for the Pu isotopic CRMs included in this investigation.

CRMs are used to establish the traceability of the analytical data to national and international measurement databases and to ensure that laboratory measurements are free from systematic biases. In nuclear material control and accountability measurements, which are used to quantify nuclear material inventories, assurance of accuracy (demonstration of the absence of biases) is of utmost importance because the material quantities have significant safeguards and safety implications. Analytical instruments underwent far-reaching improvements since the initial NBS characterization studies of SRMs. Analytical methods have also been developed to take advantage of the improved performance of the instrumentation (*i.e.*, better detection capabilities and automatic instrument operation). The cumulative effect of the changes in the analytical methods and associated instrumentation was an order-of-magnitude improvement in the quality of isotope amount ratio measurements *via* mass spectrometry relative to performance levels in the initial SRM characterization measurements. The referenced literature[51] provides a more detailed discussion of the need for standards with better uncertainties to support nuclear forensics investigations of U and Pu materials. In routine TIMS measurements, standards used for instrument calibration (quantifying the mass fractionation correction) often account for more than 90% of the uncertainty in the measurement results.[53] The standards needed for nuclear forensics investigations, especially those for the analyte U,[11] have received greater attention recently, and JRC-Geel has produced some

particle standards that contain trace amounts of analytes of interest in support of nuclear forensics investigations[54,55] of environmental samples.

Because of the ability to work with increasingly smaller quantities of SNMs for high-fidelity measurements that involve element contents using the isotope dilution mass spectrometry (IDMS) technique, multicollector TIMS and inductively coupled plasma mass spectrometry (ICP-MS) instruments have played a dominant role in developing and refining analytical techniques that support nuclear forensics investigations. Using quality control (QC) data associated with routine measurements of Pu in support of various programmatic customers (including nuclear forensics investigations), this study demonstrates that TIMS remains the gold standard in isotope amount ratio measurements.

Experimental techniques

Purification of the Pu fraction

The Pu fraction for isotope amount ratio measurements using TIMS/ICP-MS instruments needs separation from isobaric interferences and from other elements present in the sample matrix that may adversely influence the ionization of Pu in the instrument. Two isobaric interferences relevant for Pu isotope ratio measurements using TIMS/ICP-MS instrumentation are (1) ^{238}U produced from the decay of ^{242}Pu (or ^{238}U in natural background and in common laboratory reagents) interfering at ^{238}Pu and (2) ^{241}Am produced from the decay of ^{241}Pu interfering at ^{241}Pu. For the purification of the Pu isotopic fraction used for TIMS isotopic analyses, the general process is as follows. The Pu polymeric species are dissociated *via* fuming in concentrated HNO_3 (16 mol L^{-1}), and Pu metal samples are dissolved in HCl (12 mol L^{-1}). For Pu isotopic analyses, approximately 20 µg of the dissolved Pu solution is used for the separations as described here. The Pu solution is fumed in HNO_3 and transferred to a prepared anion-exchange column (a Nalgene-type disposable dropper plugged with a small ball of quartz wool and a water slurry of Lewatit MP5080 macroporous resin and conditioned with 4 mL of 12 mol L^{-1} HCl). The referenced literature[56,57] provides additional details on the separation chemistry of Pu. The Am is removed using 12 mol L^{-1} HCl, leaving the Pu, U, Np, and Ga sorbed as chloride complexes on the resin. The Pu is reduced to Pu(III) and is eluted with a mixture of acids (12 mol L^{-1} HCl + 0.2 mol L^{-1} HI) while the Np, U, and Ga remain sorbed on the column. In the separation procedure described above, plutonium is fully recovered (~100% recovery, as demonstrated in isotope dilution mass spectrometry experiments where a known amount of an isotopic tracer is added as the spike and the amount of the recovered spike after the separation process is monitored). For plutonium, procedural blanks remained in the <0.01 ng range.

Instrumental analysis for the isotope ratio

For Pu isotope amount ratio measurements using TIMS instrumentation, approximately 20 ng of Pu is loaded onto zone refined Re filament ribbons as a microliter drop and dried at

This journal is © The Royal Society of Chemistry 2025

J. Anal. At. Spectrom., 2025, **40**, 1879–1901 | **1881**

600 mA (the current is maintained for 2 min, or until the drop completely evaporates) followed by 1000 mA (for 2 min). In accordance with the recommendations in the ASTM Test Method C1672-23,[58] the Pu loads on the filament are conditioned *via* successive heating at 1500 mA and 2000 mA for 10 s.

The instrumental analysis followed the total evaporation (TE) methodology using the double-filament configuration, as described in previous studies.[58–63] In this configuration, a filament with the sample (evaporation filament) is placed next to a filament with no sample (ionization filament) on the sample turret. In the source housing of the TIMS instrument, the ionization filament is taken to a current of approximately 5500 mA. After peak centering and the optimization of the source lens voltages using the ^{187}Re signal, the evaporation filament current is slowly increased until an approximately 100 mV summed (^{239}Pu + ^{240}Pu) signal is obtained. Peak centering and source lens voltage optimization for the Pu mass range are then performed. The evaporation filament current is increased, under computer control, to maintain a summed (^{239}Pu + ^{240}Pu) isotopic intensity of approximately 6 V. The referenced literature[63,64] provides additional details on the TE analysis of Pu. The TE method is regarded as a state-of-the-art analytical technique for Pu, U, and Am major isotope amount ratio measurements using TIMS instruments.[58–65]

Evaluation of the TE-TIMS isotope amount ratio data

TE-TIMS instrumental analysis often utilizes an auto sequence that consistently implements the preheating steps described above for each sample/standard. The Triton TIMS instrument can analyze up to 21 samples/standards in an auto sequence using the same preset preheating, instrument calibration, and detector settings. Raw data collected by the instrument during sample analyses are exported into custom spreadsheets validated using a software quality assurance program. Both the major and minor isotope amount data are corrected for mass fractionation effects based on the difference between the measured major isotope ratio and the certified ratios of a traceable standard. For Pu, certified ratios decay-corrected to the date of purification of the Pu isotopic fraction are compared with the measured ratios. The standard used for estimating the mass fractionation correction in TE-TIMS analysis is known as the comparator standard. This correction is performed on a per turret basis using aliquots of the same standard distributed across the measurement sequence to better capture the change in the mass fractionation during the measurement sequence.

In addition to corrections for mass fractionation effects, the U and Pu minor isotope ratios require corrections for tailing from the major isotopes. The approach of performing tailing corrections at the Pu minor isotope amount ratios using systematic biases observed in traceable standards with similar isotopic abundances to the unknown sample yields uncertainties lower than those obtained by subtracting the tailing effects using the manufacturer-specified abundance sensitivity.[46] Additionally, the performance of these tailing corrections on a per turret basis captures the variability in the run conditions of the samples/standards, thereby making the minor

isotope amount ratio uncertainties more realistic. Corrections based on abundance sensitivity leave an undesirable residual bias at the minor isotope ratios.[46] For the data presented herein, the tailing corrections at the minor isotope ratios were performed using the approach described in detail in the referenced literature.[46]

Other factors that influence the realized uncertainties in TE-TIMS data are (i) whether analyte ionization occurs at low temperature or high temperature; (ii) variability of the ionization temperatures for the same filament current; (iii) filament backgrounds which influence analyses of low amounts of the analytes, and (iv) consistency in the filament loading conditions.

Mass fractionation correction in TE analysis

Measured isotope amount ratios from TIMS instrumentation require corrections for systematic biases arising from mass fractionation. Mass fractionation in TIMS analyses is the result of the lighter isotopes preferentially evaporating from the filament surface earlier than the heavier isotopes. The mass fractionation correction for the $n(^{235}\text{U})/n(^{238}\text{U})$ major ratio using a certified standard is represented by using eqn (1):

$$\text{mass fractionation} = \frac{(n^{235}\text{U}/n^{238}\text{U})_{\text{certified}}}{(n^{235}\text{U}/n^{238}\text{U})_{\text{measured}}}. \quad (1)$$

The mass fractionation correction per atomic mass unit (u) from the $n(^{235}\text{U})/n(^{238}\text{U})$ major isotope amount ratio is scaled appropriately to the other (minor) isotope amount ratios. For two isotopes evaporating from a hot surface with masses m_1 and m_2, the Langmuir equation (eqn (2)), which describes the vapor pressure, can be used as an approximation for the fractionation coefficient (β).

$$\beta = \sqrt{\frac{m_1}{m_2}} \quad (2)$$

Mass fractionation in TIMS measurements depends on the amount loaded on the filament, the chemical form of the analyte on the filament, the analysis configuration (single, double, or triple), the temperature at which ionization occurs, the presence or absence of ionization enhancers, and the rate of analyte evaporation from the filament surface. Even for an auto sequence analysis with the same preset analysis conditions before data collection, exact reproduction of all these analysis conditions from one filament to another is not possible. Therefore, mass fractionation is recognized as a systematic effect that is variable. Graham's law of effusion has also been used to describe fractionation in TIMS isotope ratio measurements.

In the following sections, the β values for the analytes Ga, U, Am, and Pu, as obtained from eqn (2), are compared with analytical data in isotope amount ratio measurements using the TE methodology. In quantifying and interpreting the significance of the systematic biases in the Pu (and U) isotope ratios of CRM standards, it is important to rule out the possibility that

1882 | *J. Anal. At. Spectrom.*, 2025, **40**, 1879–1901

This journal is © The Royal Society of Chemistry 2025

such biases are not caused by the variability of the mass fractionation correction factor during the instrumental analysis. Therefore, a comparison of the mass fractionation effects on the various analytes is relevant for this discussion.

Isotope amount ratio measurements for Ga

For Ga, two naturally occurring isotopes exist: ^{69}Ga and ^{71}Ga. SRM 994, the isotopic standard for Ga, is a traceable standard available from NIST as a high-purity material. SRM 994 dissolved in 1 mol L^{-1} HNO$_3$ and analysed by TIMS instrumentation is used to estimate the mass fractionation correction at the $n(^{69}\text{Ga})/n(^{71}\text{Ga})$ isotope ratio.

Because Ga is highly volatile, the TE analysis of this analyte uses a single-filament configuration. TE analysis using the single-filament configuration with approximately 20 to 30 ng of Ga is efficient for Ga isotopic analysis using TIMS instruments. Fig. 1 shows the $n(^{69}\text{Ga})/n(^{71}\text{Ga})$ isotope ratio profile in the TE analysis of Ga. Ratios measured in individual cycles (dotted symbols) and the sum-integrated isotope ratio (dashed line) are shown. Whereas the $n(^{69}\text{Ga})/n(^{71}\text{Ga})$ ratio in individual cycles changed by approximately 2.23% during TE analysis, the sum-integrated ratio differed from the true ($\cong$ certified) ratio by only approximately 0.32%. Using the atomic masses of the Ga isotopes, a mass fractionation correction of 0.71%/u is estimated from eqn (2). The mass fractionation (0.16%/u) shown in Fig. 1 is much smaller, reflecting the high volatility of Ga. The observed fractionation for Ga is significantly higher than those for actinide elements U, Am, and Pu. The high volatility of Ga makes the isotope amount ratio measurements unique in that Ga is routinely analysed using the single-filament configuration. By contrast, Am, U, and Pu are commonly analysed in the double-filament configuration. For all analytes (Ga, U, Pu, and

Am) TE has been demonstrated to be the preferred analysis method independent of whether the method utilizes the single filament configuration or double filament configuration.

Isotope amount ratio measurements for U

In most U materials, the abundances of four isotopes—^{234}U, ^{235}U, ^{236}U, and ^{238}U—are relevant from a nuclear forensics perspective. Among these isotopes, ^{235}U and ^{238}U are the most abundant isotopes in most materials, and the $n(^{235}\text{U})/n(^{238}\text{U})$ ratio is a diagnostic characteristic with implications for the process history and the intended end use of the material. CRM standards covering ^{235}U isotopic enrichments from depleted (^{235}U < 0.2%) to highly enriched (^{235}U ≈ 97%) are available from the NBL PO and from JRC-Geel.

Among the analytes discussed herein, the fractionation correction factor for U has received the most attention in the last 50 years. In fact, the initial characterization of the Pu isotopic SRMs 946, 947, and 948 (now renamed NBL CRMs 136, 137, and 138) at NBS used gravimetric mixtures prepared from U isotopic endmembers for quantifying the fractionation. Consequently, the correctness of the certified isotope ratios of these Pu CRMs assumes that mass fractionation correction factors are similar for U and Pu isotope ratio measurements using TIMS. The IRMM has performed commendable work in the certification of a series of U materials and in improving the uncertainties realized in U isotope amount ratio measurements by taking full advantage of the capabilities of modern TIMS instrumentation. Thus, the IRMM has certified U CRMs with uncertainties that are close to the performance limits achievable with modern TIMS instrumentation (additional details on IRMM U standards are available elsewhere[48]). Fig. 2 shows the $n(^{235}\text{U})/n(^{238}\text{U})$ major isotope ratio profile in the TE analysis of

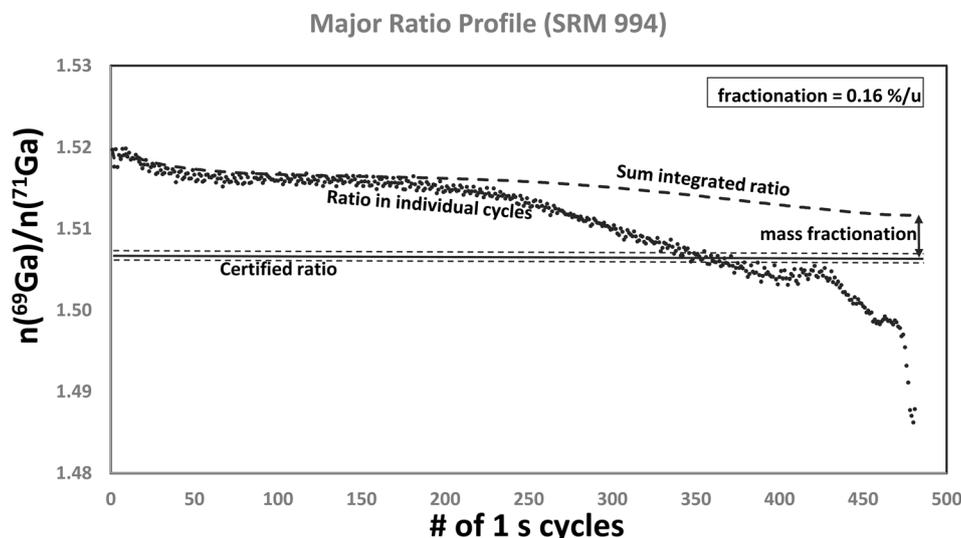**Major Ratio Profile (SRM 994)**

Fig. 1 The $n(^{69}\text{Ga})/n(^{71}\text{Ga})$ isotope ratio profile during TE analysis of SRM 994 using a Triton TIMS instrument (the solid line represents the certified ratio and the dashed lines represent the 2σ uncertainty limits on the certified ratio). While isotope ratios measured in individual cycles vary by approximately 2.2% around the certified ratio, the offset between the sum-integrated ratio and certified ratio is 0.16%/u. This offset represents mass fractionation. Even for the same loading process (by the same analyst and from the same solution bottle), the durations for which the analysis persist can be significantly different.

This journal is © The Royal Society of Chemistry 2025
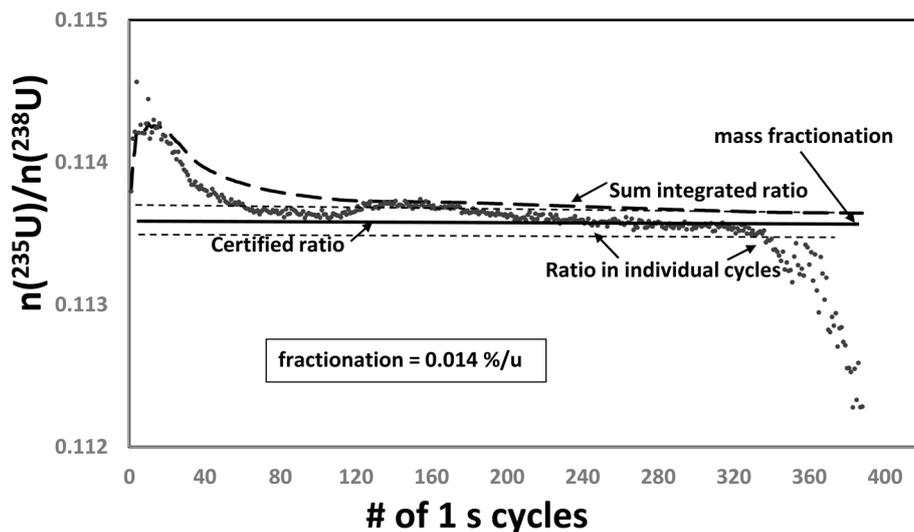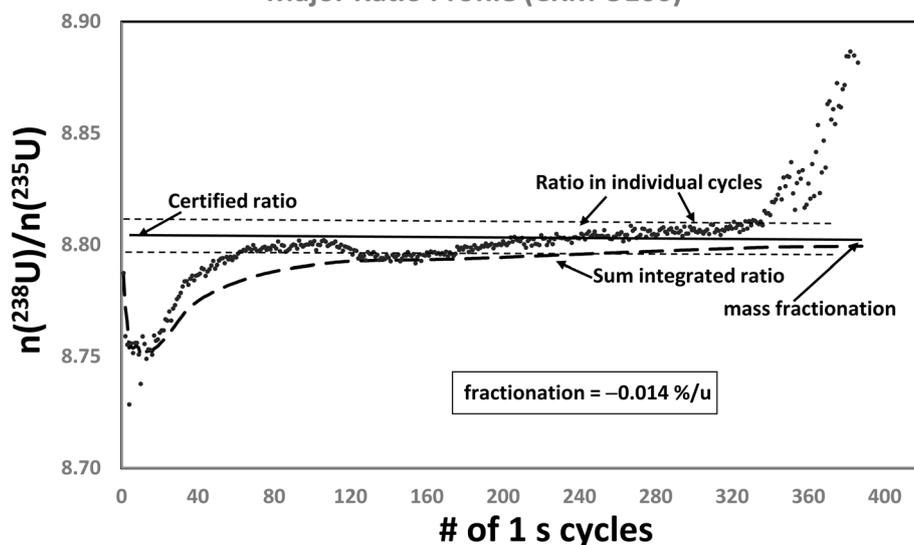
J. Anal. At. Spectrom., 2025, **40**, 1879–1901 | **1883**

Fig. 2 The $n(^{235}U)/n(^{238}U)$ isotope ratio profile during TE analysis of CRM U100 (the solid line represents the certified ratio and the dashed lines represent the 2σ uncertainty limits on the certified ratio). Measured isotope ratios in individual cycles show a variability of approximately 2% around the certified ratio. The offset between the sum-integrated ratio (at end of the TE analysis) and the certified ratio represents mass fractionation (∼0.014%/u). Even for the same loading process (by the same analyst and from the same CRM solution bottle), the durations for which the analysis persist can be significantly different.

CRM U100. During TE analysis, although the $n(^{235}U)/n(^{238}U)$ isotope amount ratio in individual cycles changed by approximately 2%, the sum-integrated ratio differed from the certified ratio by only approximately 0.042%. Notably, the deviation of the sum-integrated ratio from the certified ratio is approximately an order of magnitude smaller than that for the more volatile Ga.

As shown in Fig. 2, the heavier isotope ^{238}U, the most abundant isotope in this isotopic CRM, is used for normalization. Fig. 3 shows that if ^{235}U is used for normalization, then the mass fractionation correction factor changes sign, and the magnitude of the mass fractionation remains the same. This distinction is important because the isotope used for normalization can be heavier or lighter than the other isotopes being

Fig. 3 The $n(^{238}U)/n(^{235}U)$ isotope ratio profile during TE analysis of CRM U100 (the solid line represents the certified ratio and the dashed lines represent the 2σ uncertainty limits on the certified ratio). The same data from Fig. 2 are shown but with a different normalizing isotope. The magnitude of the mass fractionation remains the same as that in Fig. 2. However, the sign is negative, indicating that the sum-integrated ratio must be corrected upward to obtain the true ratio.

measured. Corrections for the mass fractionation effect need to be made at all isotope ratios by appropriately scaling the per-atomic mass unit fractionation.

For U, eqn (2) yields a theoretical mass fractionation correction of 0.21%/u, which is higher than the observed fractionation of 0.014%/u. Because the relative mass differences between the isotopes are similar for Am, Pu, and U, the theoretical mass fractionation corrections predicted by eqn (2) are similar for these three analytes.

Isotope amount ratio measurements for Am

For Am, two isotopes are relevant for TIMS measurements: ^{241}Am and ^{243}Am. Except for the recently certified standard from the IRMM (IRMM-0243),[65] no isotopic CRM is available for Am. Facilities have successfully implemented protocols for the production, measurement, and use of isotopic mixtures produced from endmembers ^{241}Am and ^{243}Am as working standards to estimate mass fractionation correction factors[66] in TIMS analyses of Am.

Fig. 4 shows the $n(^{241}\text{Am})/n(^{243}\text{Am})$ major isotope ratio profile in the TE analysis of Am. During TE analysis, although the $n(^{241}\text{Am})/n(^{243}\text{Am})$ isotope ratio in individual cycles changed by approximately 1.55%, the sum-integrated ratio differed from the certified ratio by only approximately 0.028%. Eqn (2) yields a mass fractionation correction factor of 0.21%/u, which is higher than the observed fractionation of 0.014%/u (Fig. 4). The per-atomic mass unit fractionation observed at the Am isotope amount ratio is comparable to that estimated from U isotope ratio measurements.

Isotope amount ratio measurements for Pu

In most Pu materials, the abundances of five isotopes—^{238}Pu, ^{239}Pu, ^{240}Pu, ^{241}Pu, and ^{242}Pu—are relevant to nuclear forensics. Among these isotopes, ^{239}Pu and ^{240}Pu are the most abundant, and the $n(^{240}\text{Pu})/n(^{239}\text{Pu})$ isotope ratio is used as the characteristic most diagnostic of the process history and intended end use of the Pu materials.[9,16,18,20] The most abundant isotope in most Pu materials is ^{239}Pu, and it is generally used as the normalizing isotope. Eqn (2) forecasts that the sum-integrated $n(^{240}\text{Pu})/n(^{239}\text{Pu})$ ratios from TE analysis should be below the certified value, as shown in Fig. 3, for the $n(^{238}\text{U})/n(^{235}\text{U})$ ratio. Fig. 5 shows the $n(^{240}\text{Pu})/n(^{239}\text{Pu})$ major isotope ratio profile in the TE analysis of CRM 136. The sum-integrated ratio at the end of TE analysis remains below the certified value, as expected from theoretical considerations for the fractionation correction when the lighter isotope is used for normalization. During TE analysis, although the $n(^{240}\text{Pu})/n(^{239}\text{Pu})$ isotope ratio in individual cycles changed by approximately 0.429%, the sum-integrated ratio differed from the certified ratio by only approximately 0.024%. The magnitude of the mass fractionation observed is smaller than the theoretical estimate of 0.21%/u using eqn (2).

The isotope profiles shown in Fig. 5–9 indicate that the sum-integrated isotopic ratio from TE indicates systematic biases in the $n(^{240}\text{Pu})/n(^{239}\text{Pu})$ major isotope ratio between the different Pu CRMs. The $n(^{240}\text{Pu})/n(^{239}\text{Pu})$ isotope ratio in individual cycles changed by 0.418%, 0.48%, and 0.529% for CRMs 137, 126-A, and 138, respectively. For CRM 128, the $n(^{242}\text{Pu})/n(^{239}\text{Pu})$ major isotope amount ratio changed by 0.957% during TE analysis. While the changes in isotope ratios are expressed on
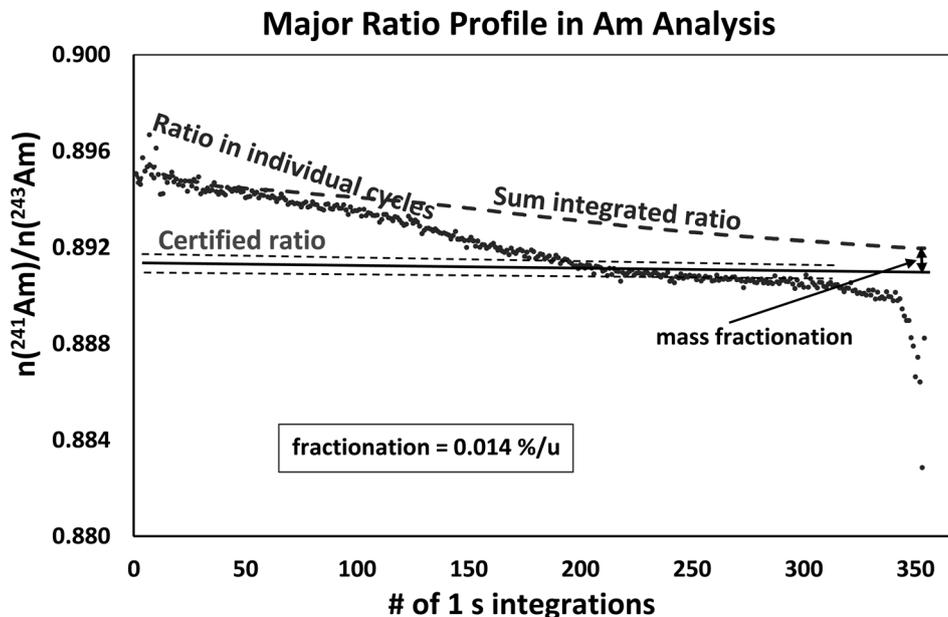

Fig. 4 The $n(^{241}\text{Am})/n(^{243}\text{Am})$ isotope ratio profile during TE analysis (the solid line represents the certified ratio and the dashed lines represent the 2σ uncertainty limits on the certified ratio). Isotope ratios measured in the individual cycles show a variability of approximately 1.5% around the true ratio. The offset between the sum-integrated ratio (at the end of TE analysis) and the true ratio represents mass fractionation. Even for the same loading process (by the same analyst and from the same standard/sample solution bottle), the durations for which the TE analysis persist can be significantly different.

This journal is © The Royal Society of Chemistry 2025

J. Anal. At. Spectrom., 2025, **40**, 1879–1901 | **1885**
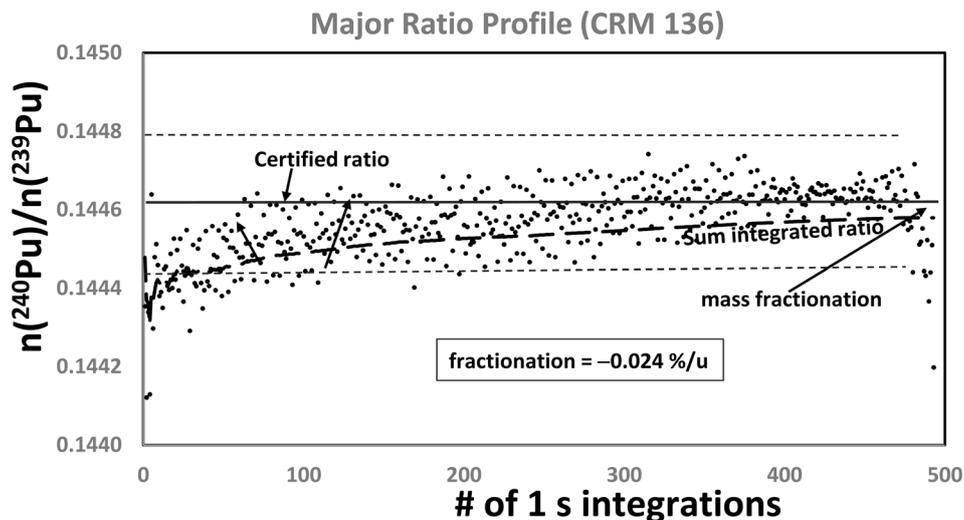
Major Ratio Profile (CRM 136)

Fig. 5   The $n(^{240}\text{Pu})/n(^{239}\text{Pu})$ isotope ratio profile during TE analysis of CRM 136 (the solid line represents the certified ratio and the dashed lines represent the 2σ uncertainty limits on the certified ratio). Whereas the sum-integrated isotopic ratio (at the end of TE analysis) remains below the certified ratio (as expected for a ratio for which the lighter isotope is used as the normalizing isotope), the magnitude of the mass fractionation correction (estimated using CRM 136) is marginally larger than those observed for U and Am.

a 1 u basis for CRMs 136, 137, 138, and 126-A, the change for CRM 128 is 3 u.

The differences in the magnitude of the mass fractionation estimated from the different Pu standards represent small systematic differences (biases) between the Pu CRMs. Systematic biases of similar magnitude (between different U CRMs) were identified for the $n(^{235}\text{U})/n(^{238}\text{U})$ major isotope ratio (as shown in Fig. 10) when the modified total evaporation (MTE) method[67,68] was developed and applied to characterization efforts of U isotopic CRMs from the NBL PO. Fig. 10 shows that

systematic biases of up to $\pm 0.05\%$ were observed in specific NBL U CRMs when all standards were normalized to CRM U500. Notably, when these NBL U (and Pu) CRMs were initially characterized, advanced analytical techniques, such as TE, were not available; TIMS instrumentation and analytical methodologies have evolved significantly in the 30 years since the initial characterization of these standards. In an excellent demonstration of the knowledge and proficiency of the NBS metrologists and the versatility of the first-generation mass spectrometry instruments used to certify these standards, the
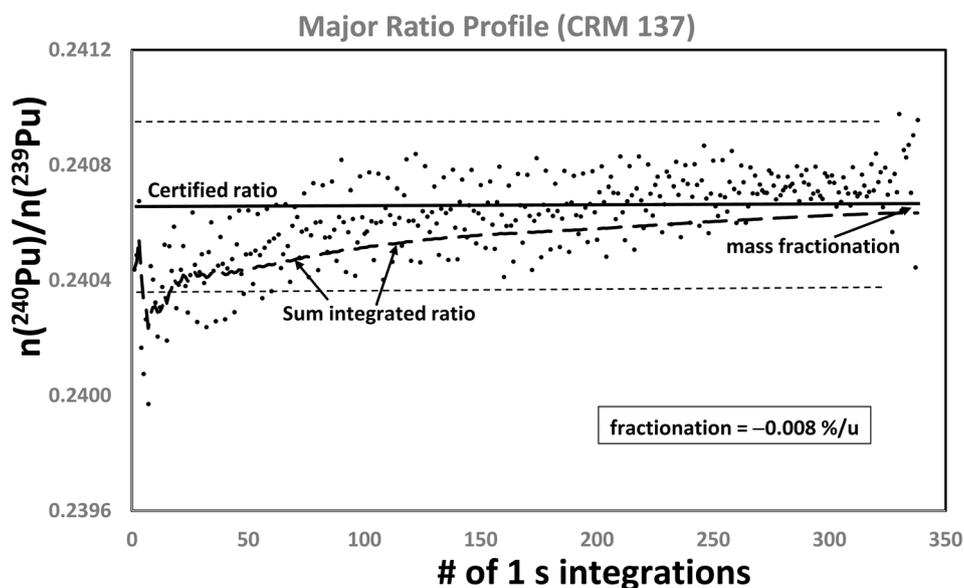
Major Ratio Profile (CRM 137)

Fig. 6   The $n(^{240}\text{Pu})/n(^{239}\text{Pu})$ isotope ratio profile during TE analysis of CRM 137 (the solid line represents the certified ratio and the dashed lines represent the 2σ uncertainty limits on the certified ratio). The sum-integrated isotopic ratio (at the end of TE analysis) remains below the certified ratio (as expected for a ratio for which the lighter isotope is used as the normalizing isotope). The magnitude of the mass fractionation correction is slightly smaller than that estimated using CRM 136.
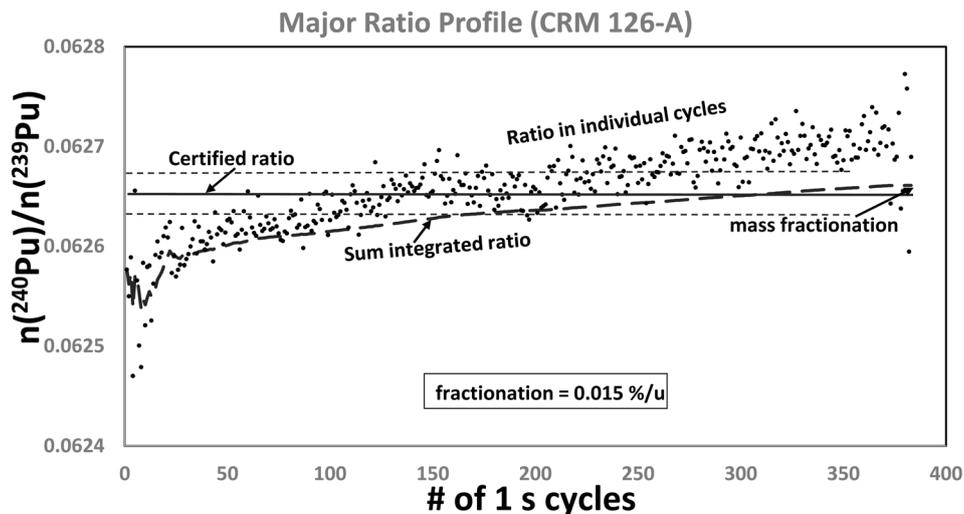
Fig. 7 The $n(^{240}Pu)/n(^{239}Pu)$ isotope ratio profile during TE analysis of CRM 126-A (the solid line represents the certified ratio and the dashed lines represent the 2σ uncertainty limits on the certified ratio). The sum-integrated isotopic ratio (at the end of TE analysis) is above the certified ratio, contrary to what is expected for a ratio for which the lighter isotope is used as the normalizing isotope.

certified isotope ratios of the NBS U and Pu SRMs have stood the test of time. The improved precision and accuracy achieved by modern TIMS instrumentation enable the identification of systematic biases greater than or equal to $\pm0.02\%$ in the major isotope ratios.[69] This is especially true for Pu isotopic CRMs because the characterization of the Pu isotopic standards preceded most of the U CRMs characterized by NBS/NBL. Also of note is that during the initial certification of SRMs 946, 947, and 948, gravimetric mixtures produced from ^{235}U and ^{238}U were used to estimate the mass fractionation effects in TIMS isotope ratio measurements.

Among other parameters, the mass fractionation correction factor in TIMS analyses depends on the amounts of the element loaded on the filaments, the chemical form of the element, and the current at which the element is evaporated from the filament surface. During the initial NBS characterization, the effect of these factors on the magnitude of the mass fractionation correction factor and the precision of the correction factor were investigated in great detail.[50] Fractionation factors associated with both high-temperature and low-temperature evaporation from the filaments were investigated in detail during the initial NBS characterization. For the analytical data presented herein,
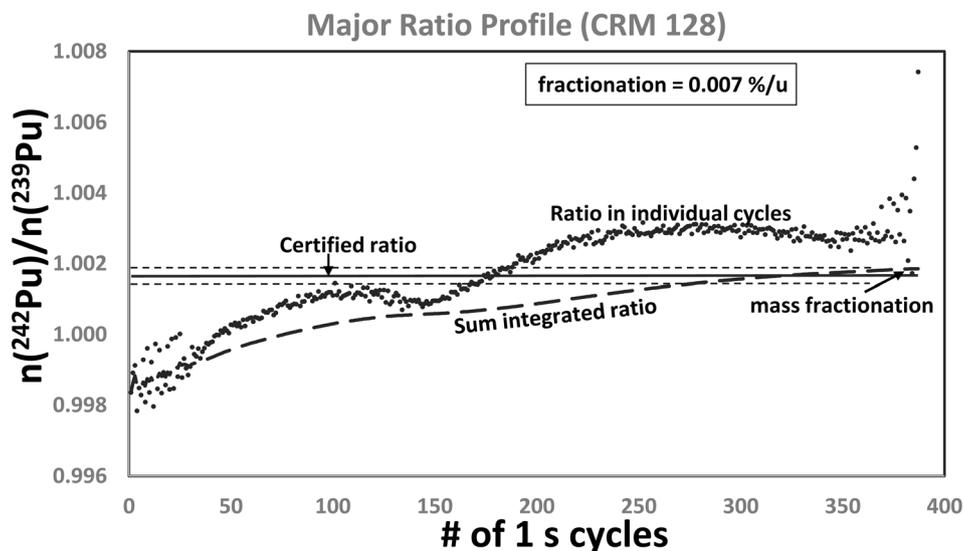

Fig. 8 The $n(^{242}Pu)/n(^{239}Pu)$ isotope ratio profile during TE analysis of CRM 128 (the solid line represents the certified ratio and the dashed lines represent the 2σ uncertainty limits on the certified ratio). The sum-integrated isotopic ratio (at the end of TE analysis) is above the certified ratio, contrary to what is expected for a ratio for which the lighter isotope is used as the normalizing isotope. Notably, the fractionation observed for CRM 128 is similar to that for CRM 126-A, and CRM 128 was used as the standard for estimating mass fractionation in CRM 126-A certification analyses.
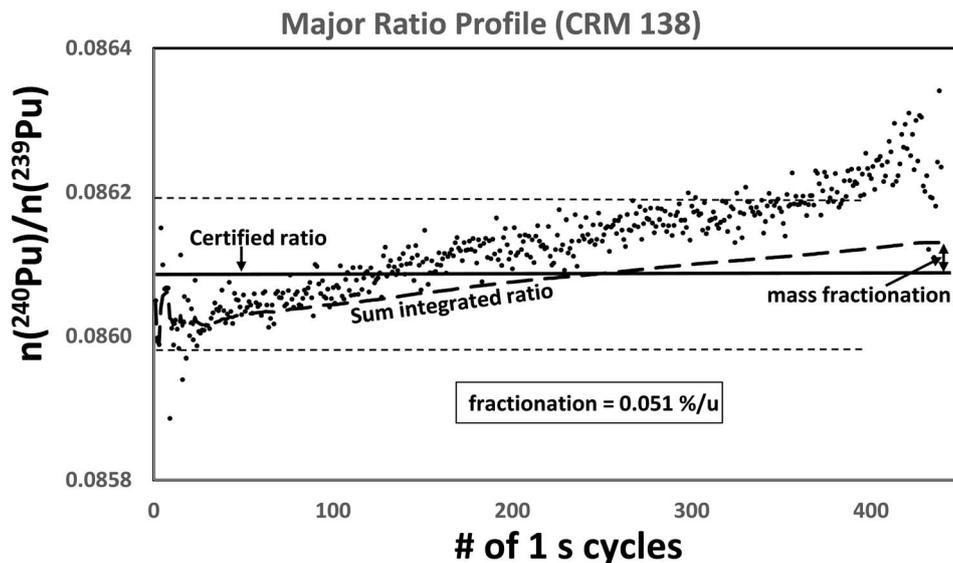
Fig. 9 The $n(^{240}Pu)/n(^{239}Pu)$ isotope ratio profile during TE analysis of CRM 138 (the solid line represents the certified ratio and the dashed lines represent the 2σ uncertainty limits on the certified ratio). The sum-integrated isotopic ratio (at the end of TE analysis) is above the certified ratio, contrary to what is expected for a ratio for which the lighter isotope is used as the normalizing isotope. The mass fractionation correction is significantly larger than what has been observed in any of the Pu isotopic standards. Literature data on this standard indicate that the major isotope ratio is systematically biased.[64]

the same amounts of the NBS/NBL Pu isotopic CRMs were analyzed following the same analytical routines for sample loading and for instrumental analyses. Therefore, similar mass fractionation corrections (per atomic mass unit) are expected from the different CRMs (136, 137, 138, 126-A, and 128), and the differences in the fractionation factors most likely represent systematic biases in the major isotope ratio of these standards.

Fig. 11 shows the relative deviations of the major isotope ratio for Pu CRMs 136, 137, and 138 from the certified ratios (published data from Romkowski *et al.*[59] are shown). These are the first analytical data available in the literature for Pu isotopic standards analyzed using a TE methodology. A key difference to note is that whereas the isotopic data shown for the U standards in Fig. 10 have been corrected for mass fractionation using the measured $n(^{235}U)/n(^{238}U)$ isotope amount ratio in CRM U500,
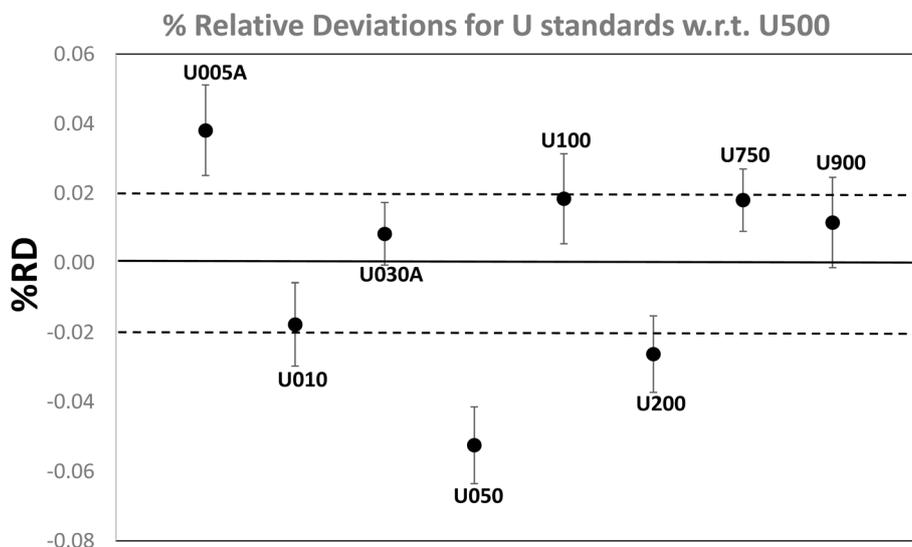

Fig. 10 Relative deviations of the major isotope amount ratios (using CRM U500 as the comparator), as reported by Richter and Goldberg[67] from certified ratios of U CRMs from the NBL. The solid line represents the bias-free data and the dashed lines indicate uncertainty limits typical for recently certified U standards from the IRMM and limits that can be achieved through the use of state-of-the-art analytical techniques like TE and MTE.[61,68] Using CRM U005A or U050 as the comparator standard can bias the major isotope ratios outside the certified uncertainty limits of the IRMM standards. Error bars on individual CRMs indicate the within turret precision ($n = 4$ or more data points) measured in MTE experiments.
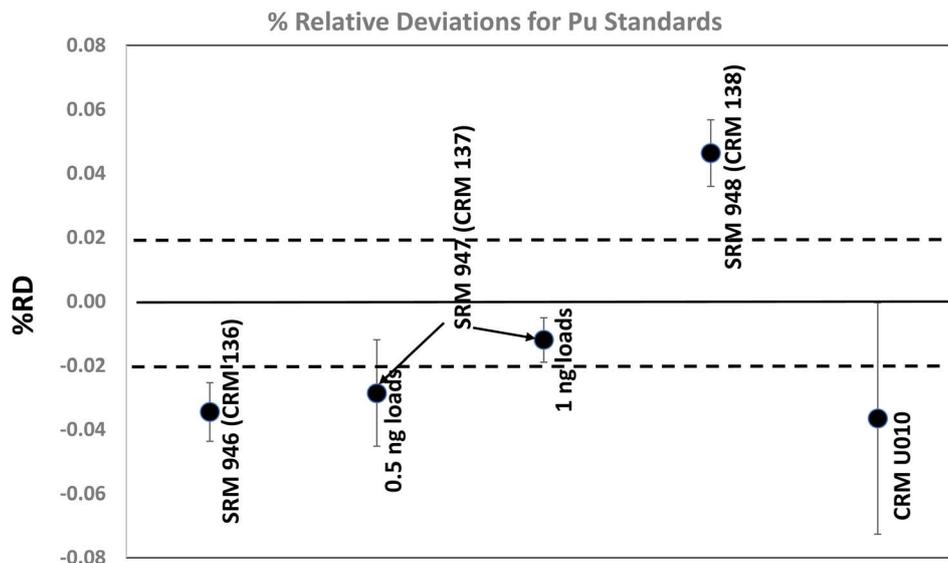
1888 | *J. Anal. At. Spectrom.*, 2025, **40**, 1879–1901

This journal is © The Royal Society of Chemistry 2025

Fig. 11 Relative deviations of the measured $n(^{240}\text{Pu})/n(^{239}\text{Pu})$ isotope ratios in Pu CRMs 136, 137, and 138 (data reported by Ramkowski *et al.*[59]). This was the first demonstration that the TE technique can be used to improve the Pu major isotope ratio measurements using TIMS instruments. The solid line represents bias free data and the expanded uncertainties that correspond to the limits achieved using modern TIMS instruments (by the TE technique) for major isotope ratio measurements on Pu, U, or Am are shown for comparison. To be consistent with the Pu isotope ratio, for which the lighter isotope is used for normalization, the $n(^{238}\text{U})/n(^{235}\text{U})$ ratio with the lighter isotope normalization is shown for U010.

the Pu data shown in Fig. 11 are not corrected for mass fractionation effects. Average measured isotope ratio values and standard errors for 10 independent measurements are shown in Fig. 11. Whereas CRMs 136 and 137 indicate fractionation corrections comparable to that in U010, CRM 138 indicates fractionation correction in the opposite direction because this standard is on the other side of the zero line. For the U010 data shown in Fig. 11, the major isotope ratio is expressed as $n(^{238}\text{U})/n(^{235}\text{U})$ to make the lighter isotope the normalizing isotope comparable with the normalization for the Pu standards.

As discussed, fractionation effects have been investigated more extensively for U because of extensive certification efforts at NBS during the production of the U-series SRMs, recent certification efforts at the IRMM[48] and NBL, and the development of the MTE technique.[67,68] The MTE technique is superior in that it concurrently provides both major and minor U isotope ratios by simultaneously applying the TE principle and the systematic measurement of the tailing effects (close to half-masses) on either side of the minor isotope signal. This strategy allows the tailing corrections to be performed with greater precision. The MTE technique was also used in the recent certification efforts at the NBL for CRMs 115, 112-A, 125-A, and 116-A. A previous study[69] provides summary data on recent U standards certified by the NBL and a discussion of the uncertainties suggested to be achievable in analytical labs using TIMS instrumentation and the MTE technique.

The $n(^{235}\text{U})/n(^{238}\text{U})$ major isotope ratios shown in Fig. 10 are corrected for mass fractionation effects, whereas the $n(^{240}\text{Pu})/n(^{239}\text{Pu})$ isotope ratios shown in Fig. 11 are not corrected for mass fractionation effects. If corrected for mass fractionation effects using CRM 136, then the CRM 138 data will be pushed higher to a percent relative deviation value of approximately

0.08%, which is consistent with the bias reported in the literature[64] for this CRM standard.

Evaluation of the Pu isotope ratio uncertainties

QC data generated as part of routine measurement efforts in support of various programmatic customers were statistically evaluated to estimate the uncertainties realized in Pu isotope amount ratio measurements using TIMS instrumentation. QC data covering a time interval of 5.5 years were used for this evaluation. During a short (compared to the half-lives of the respective isotopes) time interval such as 5 years, the $n(^{240}\text{Pu})/n(^{239}\text{Pu})$ major isotope ratio changed only slightly because of the longer half-lives of ^{239}Pu (24 119 years) and ^{240}Pu (6564 years).[70] However, the minor isotope ratio such as $n(^{241}\text{Pu})/n(^{239}\text{Pu})$ changed substantially during this time interval.

Although control charts for the $n(^{240}\text{Pu})/n(^{239}\text{Pu})$ major isotope ratios for all CRMs were evaluated in detail, no such evaluation was attempted for the $n(^{238}\text{Pu})/n(^{239}\text{Pu})$, $n(^{241}\text{Pu})/n(^{239}\text{Pu})$, and $n(^{242}\text{Pu})/n(^{239}\text{Pu})$ minor isotope amount ratios because these ratios are affected by tailing corrections. For the Pu minor isotope ratios, an evaluation using control charts of isotopic data corrected for tailing effects using different correction methodologies for the biases resulting from tailing has been presented elsewhere.[46]

Uncertainty in the $n(^{240}\text{Pu})/n(^{239}\text{Pu})$ major isotope ratio

As discussed, the $n(^{240}\text{Pu})/n(^{239}\text{Pu})$ isotope amount ratio is fundamental for attribution of the source and intended use of Pu materials. This isotope ratio has the smallest uncertainties associated with it (as reflected by the smaller ITV-2020 (ref. 71) values for this ratio) compared with other Pu isotope ratios,
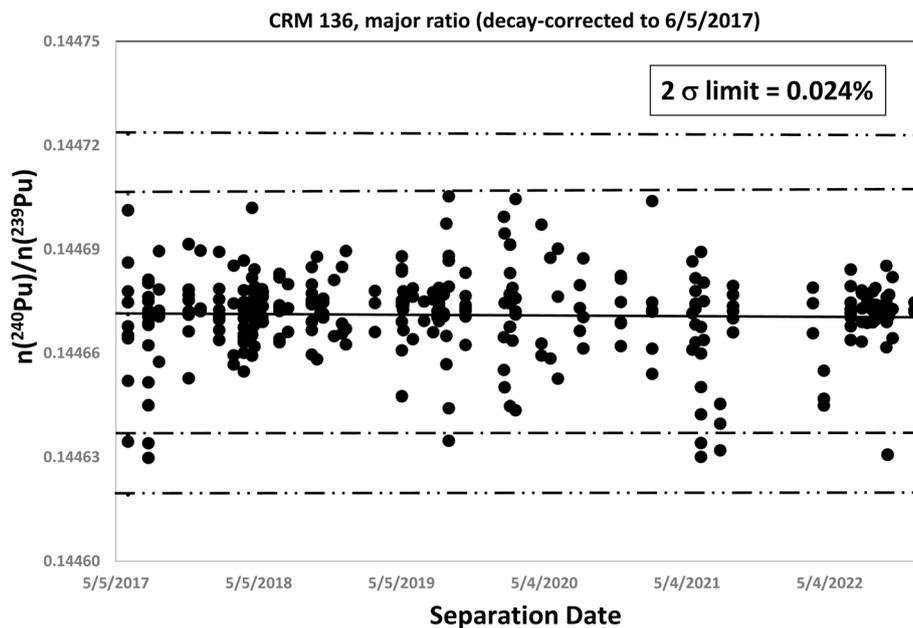
Fig. 12 Plot of the $n(^{240}\text{Pu})/n(^{239}\text{Pu})$ ratio (decay-corrected to 6/5/2017) in high-burnup (fuel-grade) Pu isotopic standard CRM 136. The solid line represents the average isotope ratio and both the 2-s and 3-s uncertainty limits for the data set are represented by the dashed lines. An expanded uncertainty representing a 95% confidence interval of 0.024% (using a coverage factor of $k = 2$) is obtained for this isotopic standard.

indicating its importance for deciphering the intended use of the Pu material in question. In fact, one of the major motivations for developing TIMS analytical methodologies, such as TE, has been to improve the precision, accuracy, and resulting combined uncertainty of the $n(^{240}\text{Pu})/n(^{239}\text{Pu})$ and the $n(^{235}\text{U})/n(^{238}\text{U})$ major isotope ratios.

The $n(^{240}\text{Pu})/n(^{239}\text{Pu})$ major isotope ratios, decay-corrected to a common date (chosen to be the same as the first measurement indicated in the dataset), were control-charted to estimate the uncertainties realized for the major isotope ratio by the TE methodology. Fig. 12 shows a plot of the major isotope amount ratio data in the high-burnup (fuel-grade) standard CRM 136. A
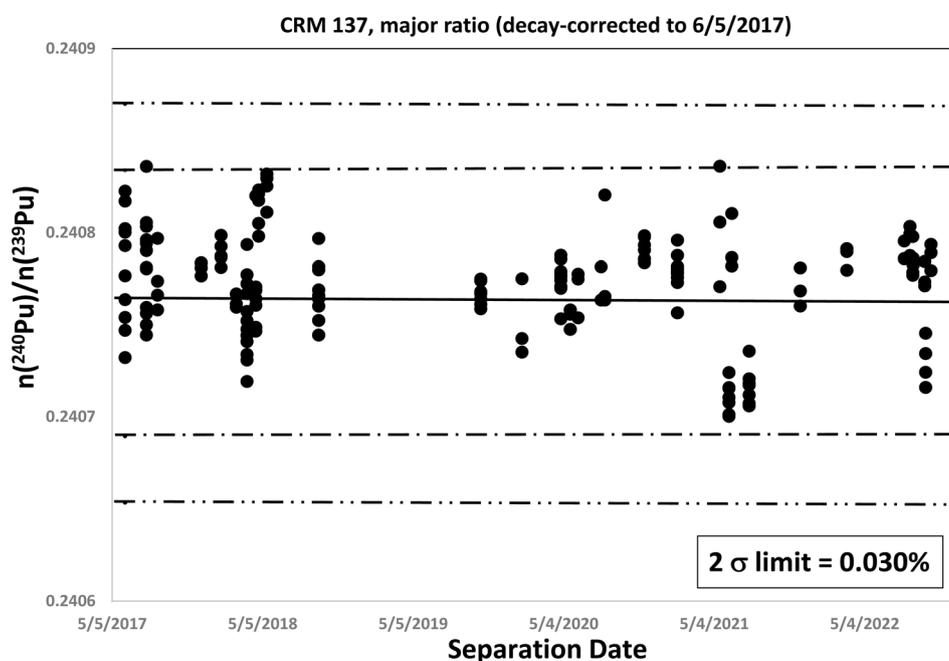

Fig. 13 Plot of the $n(^{240}\text{Pu})/n(^{239}\text{Pu})$ ratio (decay-corrected to 6/5/2017) in high-burnup (reactor-grade) Pu isotopic standard CRM 137. The solid line represents the average isotope ratio and both the 2-s and 3-s uncertainty limits for the data set are represented by the dashed lines. An expanded uncertainty representing a 95% confidence interval of 0.030% (using a coverage factor of $k = 2$) is obtained for this isotopic standard.

1890 | J. Anal. At. Spectrom., 2025, **40**, 1879–1901

This journal is © The Royal Society of Chemistry 2025

2σ warning limit, corresponding to a 95% confidence interval of 0.024%, was obtained for the $n(^{240}\text{Pu})/n(^{239}\text{Pu})$ major ratio of CRM 136 using the long-term QC dataset covering approximately 5.5 years of analytical data for this standard. Two data points (representing 0.57% of the data) plotted between the 2σ and 3σ limits indicate that the uncertainty limits estimated are not overly conservative and are appropriate for the dataset.

Fig. 13 shows a plot of the major ratio data (decay-corrected to the date corresponding to the first data point in the dataset) in the high-burnup (reactor-grade) standard CRM 137. A 2σ warning limit, corresponding to a 95% confidence interval of 0.030%, was obtained for the $n(^{240}\text{Pu})/n(^{239}\text{Pu})$ major ratio of CRM 137 using the QC dataset covering more than 5 years. The slightly larger limit for CRM 137, compared with that of CRM 136, can be attributed to the fewer number of measurements for this isotopic standard.

Fig. 14 and 15 show the major ratio data in low-burnup standards CRM 138 (fuel-grade material) and CRM 126-A (weapons-grade material). QC data from both of these low-burnup CRMs are consistent with a 2σ warning limit, corresponding to a 95% confidence interval of 0.030%. For all four CRMs, the estimated 2σ limits represent the expanded uncertainties that can be realized in a single measurement using TIMS instrumentation and a coverage factor of $k = 2$.

Fig. 16 shows the uncertainty budget for the $n(^{240}\text{Pu})/n(^{239}\text{Pu})$ major isotope ratio. Precision of the isotope ratio measurement dominates the uncertainty budget: 65% of the overall uncertainty comes from this factor. The uncertainty in the major isotope ratio of the comparator standard used to quantify the fractionation correction accounts for 35% of the uncertainty budget. For the $n(^{240}\text{Pu})/n(^{239}\text{Pu})$ isotope ratio, the uncertainty budgets for all four Pu isotopic CRMs (both high- and low-

burnup Pu standards) evaluated here are similar. The uncertainty budget for the major isotope ratio obtained here is different from that estimated by Bürger et al.,[53] where more than 90% of the uncertainty was estimated to come from the uncertainty in the certified major isotope ratio of the comparator standard used for estimating the mass fractionation correction factor.

The nominal uncertainty of 0.024% to 0.030% (expanded uncertainty at the 95% confidence interval) estimated for the $n(^{240}\text{Pu})/n(^{239}\text{Pu})$ major isotope amount ratio is similar to the uncertainties assigned to the major U isotope ratios in IRMM U CRMs, demonstrating that these uncertainty limits can be achieved on a routine basis in analytical laboratories[51,67,69] with excellent quality control practices. The accuracy and precision achieved in recent NBL U CRM certification measurements indicate that the uncertainty limit is also similar to the uncertainty estimate for the $n(^{235}\text{U})/n(^{238}\text{U})$ major isotope ratio measurements.[69] This uncertainty limit also implies that for Pu and U isotopic standards, systematic biases larger than 0.03% in the $n(^{240}\text{Pu})/n(^{239}\text{Pu})$ and $n(^{235}\text{U})/n(^{238}\text{U})$ isotope ratios are statistically significant.[64] For Pu isotopic analyses, a high-intensity total evaporation (HI-TE) method[72] that has recently been developed to improve the minor isotope amount ratio uncertainties yields marginally improved performance for the $n(^{240}\text{Pu})/n(^{239}\text{Pu})$ major isotope ratio.

Uncertainty in the Pu minor isotope ratios

Among the Pu minor isotope amount ratios, tailing correction is anticipated to be the most significant factor dictating the uncertainty in the $n(^{238}\text{Pu})/n(^{239}\text{Pu})$ isotope amount ratio because the ^{238}Pu isotope is only 1 u below ^{239}Pu, which is typically the largest signal in most Pu materials. Fig. 17 shows
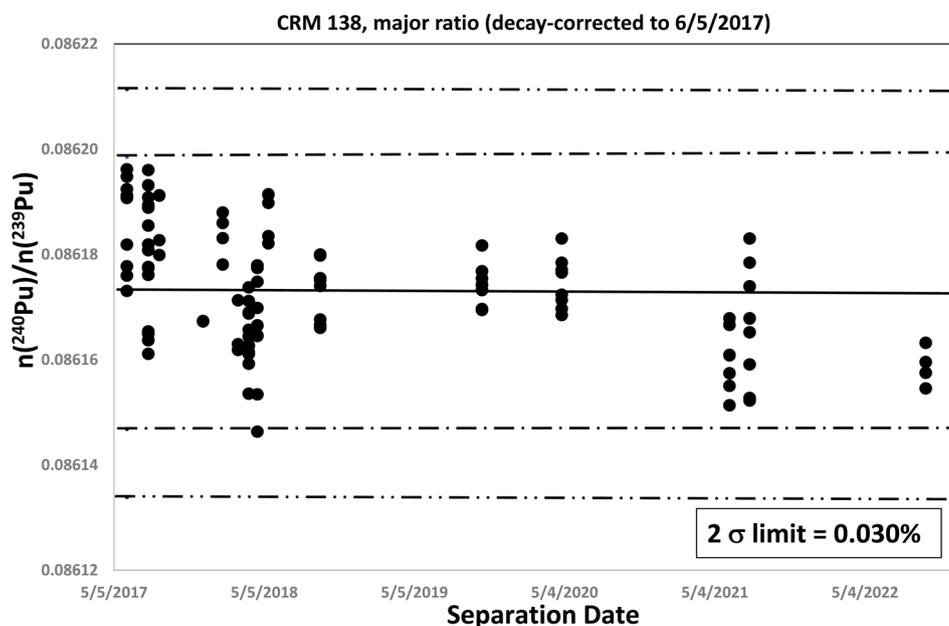
CRM 138, major ratio (decay-corrected to 6/5/2017)

2 σ limit = 0.030%

Fig. 14 Plot of the $n(^{240}\text{Pu})/n(^{239}\text{Pu})$ ratio (decay-corrected to 6/5/2017) in low-burnup (weapons-grade) Pu isotopic standard CRM 138. The solid line represents the average isotope ratio and both the 2-s and 3-s uncertainty limits for the data set are represented by the dashed lines. An expanded uncertainty representing a 95% confidence interval of 0.030% (using a coverage factor of $k = 2$) is obtained for this isotopic standard.
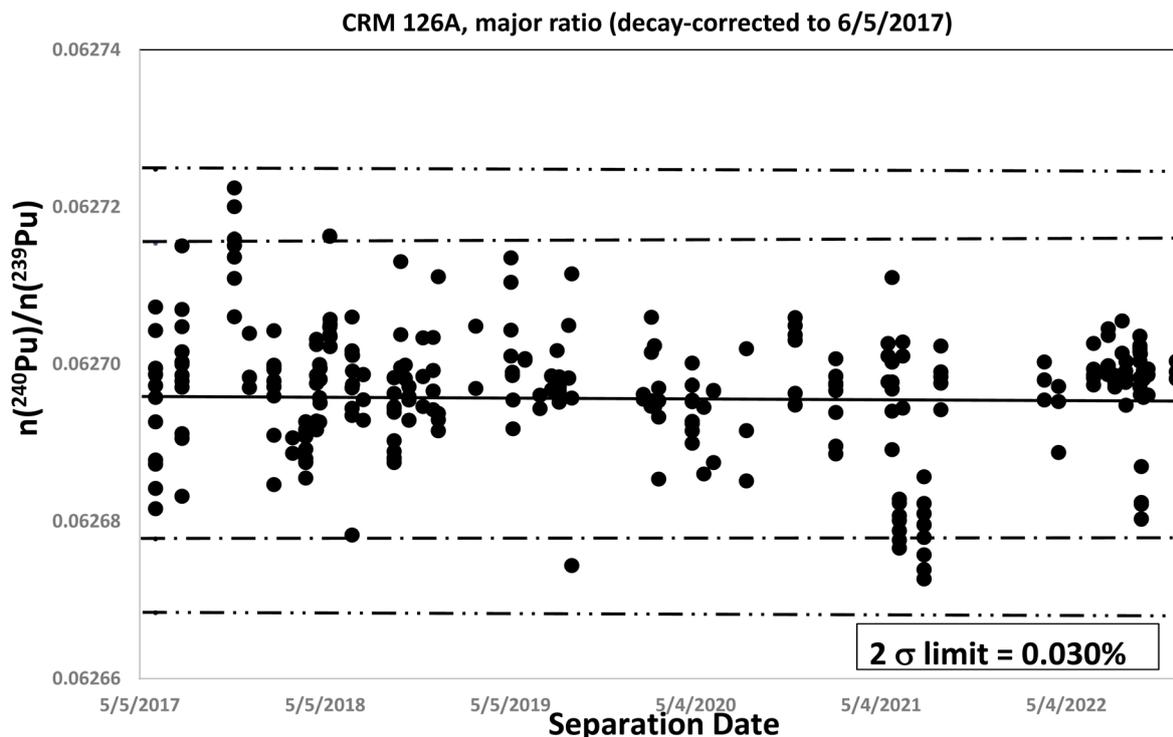
Fig. 15 Plot of the $n(^{240}\text{Pu})/n(^{239}\text{Pu})$ ratio (decay-corrected to 6/5/2017) in low-burnup (weapons-grade) Pu isotopic standard CRM 126-A. The solid line represents the average isotope ratio and both the 2-s and 3-s uncertainty limits for the data set are represented by the dashed lines. An expanded uncertainty representing a 95% confidence interval of 0.030% (using a coverage factor of $k = 2$) is obtained for this isotopic standard.

a plot of the tailing correction for the $n(^{238}\text{Pu})/n(^{239}\text{Pu})$ minor isotope ratios of CRMs 136, 137, 138, and 126-A. The tailing correction increases exponentially as the Pu material type changes from high-burnup to low-burnup and as the $n(^{238}\text{Pu})/n(^{239}\text{Pu})$ ratio decreases.

While the tailing corrections for the $n(^{238}\text{Pu})/n(^{239}\text{Pu})$ minor ratio amount to approximately 1% for the high-burnup CRMs 136 and 137, corrections greater than 10% and greater than 20% are necessary for the low-burnup CRMs 126-A and 138, respectively. Because the ^{238}Pu abundances in CRMs 126-A and 138 are approximately 10–20× smaller than those in CRMs 136 and 137,
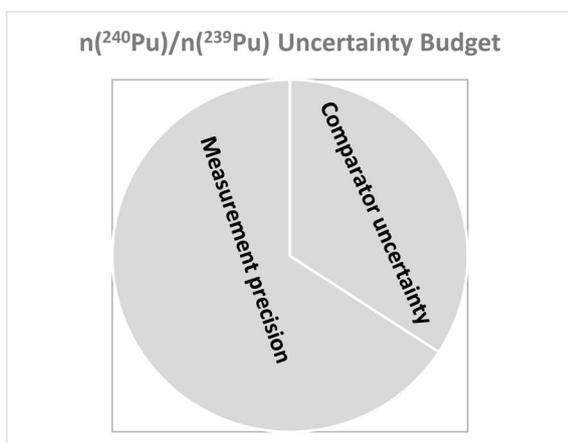

Fig. 16 Uncertainty budget for the $n(^{240}\text{Pu})/n(^{239}\text{Pu})$ major isotope ratio. An expanded uncertainty of approximately 0.030% is estimated for routine TE measurements (with a 6 V [SUM] target intensity). The precision of the isotope ratio measurement accounts for approximately 65% of the overall uncertainty, and the uncertainty in the certified ratio of the CRM standard used for quantification of the mass fractionation accounts for approximately 35% of the overall uncertainty.
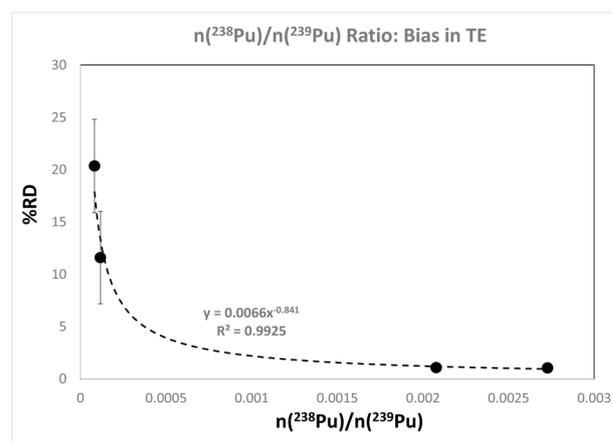

Fig. 17 Bias (resulting from tailing from the major isotopes) in the $n(^{238}\text{Pu})/n(^{239}\text{Pu})$ isotope ratio as a function of the ratio value. While for the high-burnup standards, the bias corrections are only approximately 1%, for the low-burnup standards with $n(^{238}\text{Pu})/n(^{239}\text{Pu})$ ratios less than 0.0003, the biases (and corrections) are large. These biases are also associated with large uncertainties, as indicated by the large error bars on the data points with low isotope ratio values.
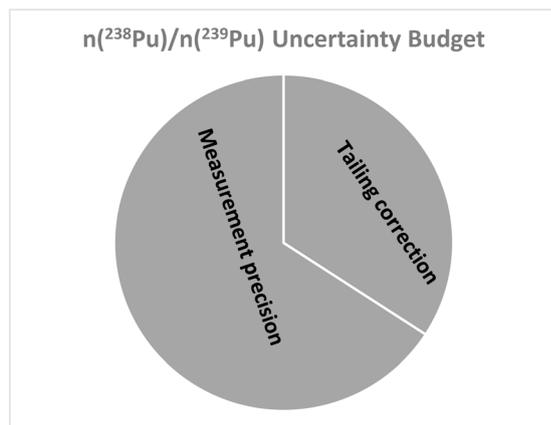
1892 | *J. Anal. At. Spectrom.*, 2025, **40**, 1879–1901

This journal is © The Royal Society of Chemistry 2025

Fig. 18 Uncertainty budget for the $n(^{238}Pu)/n(^{239}Pu)$ isotope ratio (shown as an example for minor isotope ratios). The precision of the isotope ratio measurement (accounting for 65% of the uncertainty) and the tailing correction (accounting for 35% of the uncertainty) dictate the uncertainties realized for the $n(^{238}Pu)/n(^{239}Pu)$ isotope ratio.
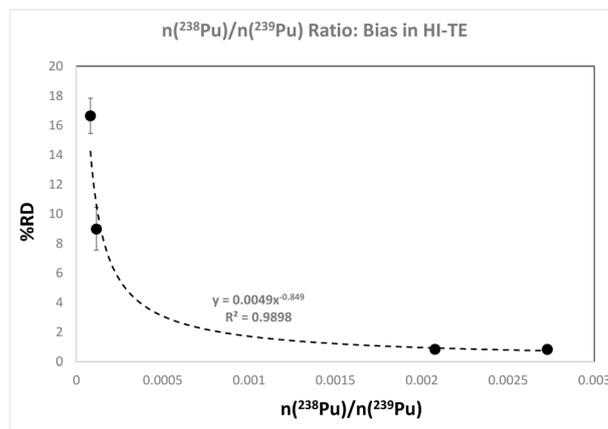

Fig. 19 Bias in the $n(^{238}Pu)/n(^{239}Pu)$ isotope ratio as a function of the ratio value for HI-TE measurements. The tailing correction is marginally smaller, and the uncertainty of the tailing correction is also smaller.

the tailing correction is a significant source of uncertainty for the $n(^{238}Pu)/n(^{239}Pu)$ isotope ratio (the variability in the isotope ratio measurement remains the larger contributor to the uncertainty budget) for low-burnup Pu materials. Performing the tailing corrections on a per-turret basis captures the variability in the tailing correction factor more accurately than making the corrections using an assumed (or measured) correction factor based on manufacturer-specified abundance sensitivity.[46] Fig. 18 shows the uncertainty budget for the $n(^{238}Pu)/n(^{239}Pu)$ minor isotope ratio using the TE methodology.

For the $n(^{241}Pu)/n(^{239}Pu)$ and $n(^{242}Pu)/n(^{239}Pu)$ isotope ratios, the observed biases resulting from tailing are less than 0.5%, and the uncertainty budgets for these isotope ratios are dominated by the precision of the isotope ratio measurements. The measured values of these isotope ratios, within the precision of the measurements, overlap the certified isotope ratios, suggesting that statistically significant corrections resulting from tailing are not present.[46] Uncertainty budgets for $n(^{241}Pu)/n(^{239}Pu)$ and $n(^{242}Pu)/n(^{239}Pu)$ are similar; the precision of the isotope ratio measurement accounts for approximately 65–70% of the overall uncertainty in the isotope amount ratio. Tailing correction accounts for the remainder of the uncertainty budget in the $n(^{241}Pu)/n(^{239}Pu)$ and $n(^{242}Pu)/n(^{239}Pu)$ isotope amount ratios. Uncertainty in the mass fractionation correction factor is not a significant contributor to the minor Pu isotope amount ratio uncertainties.

Recently, a HI-TE method has been developed. This method further improves the uncertainty in the minor isotope amount ratios.[72] In this method, approximately double the amount of Pu was loaded on the filaments (compared with the amounts mentioned in Section II for TE analysis), and a summed ($^{239}Pu + {}^{240}Pu$) target intensity of 24 V was used. The minor isotope amount ratio uncertainties achieved using the HI-TE method are substantially improved (by a factor of 2 to 3) compared with those achieved using the TE technique. Fig. 19 shows the bias in the $n(^{238}Pu)/n(^{239}Pu)$ minor isotope amount ratio using the HI-

TE method. For HI-TE measurements, the tailing corrections (as a percent) become smaller; more importantly, the uncertainty on the tailing corrections also becomes smaller. The HI-TE method can be used to obtain state-of-the-art uncertainties for Pu minor isotope amount ratios.

Demonstration of the quality of Pu isotopic data using the double ratio technique

To demonstrate the fidelity of the Pu isotope ratio measurements by TIMS, the half-life value of ^{241}Pu was estimated by the double ratio technique using the analytical data for traceable CRMs 136, 137, 138, and 126-A. Among the Pu CRMs routinely used at the Actinide Analytical Chemistry (C-AAC) group at the Los Alamos National Laboratory (LANL), the ^{241}Pu abundance in CRM 128 is at ultra trace levels (even for the HI-TE method, the ^{241}Pu isotopic signal in this standard is less than 1 mV), and this standard is not included in the half-life estimation analysis presented herein.

In principle, the ^{241}Pu half-life value can be estimated from changes in the $n(^{241}Pu)/n(^{239}Pu)$ ratio over time.[73–75] Zeigler and Ferris[75] used this approach to estimate the ^{241}Pu half-life value using data generated by six DOE laboratories (on an interlaboratory comparison standard with approximately an order-of-magnitude higher concentration of the ^{241}Pu isotope than CRM 137, the CRM with the highest ^{241}Pu abundances among the four isotopic CRMs included in this study) and estimated a value of 14.89 ± 0.11 years. Although the estimated half-life value from this investigation was determined using a Pu material with approximately an order of magnitude higher ^{241}Pu abundance than the CRM with the highest ^{241}Pu included in this study, the offset of the half-life estimate from the currently accepted value has implications for the TE method using TIMS instruments. The single isotope ratio technique that was used for the Zeigler and Ferris[75] study did not yield accurate isotope ratio results because of the nature of the analytical methodology and the analytical methodology not being based on TE. For the $n(^{241}Pu)/n(^{239}Pu)$ isotope ratio, eqn (2) implies

This journal is © The Royal Society of Chemistry 2025

J. Anal. At. Spectrom., 2025, **40**, 1879–1901 | **1893**

a fractionation correction factor of 1.00418. Therefore, variations less than or equal to 10^{-3} in the mass fractionation correction factor are sufficient to increase the uncertainty in the half-life value estimated. Fig. 5 thru 9 shows that the isotope ratios changed by several percent during the course of the Pu release from the filament. In the Zeigler and Ferris[75] study, these changes in the isotope amount ratios cause accuracy issues in the data. In the double ratio method, the decrease over time of an isotope is determined not by a single ratio but by using a suitably chosen double ratio. A detailed description of the double ratio technique is provided in the referenced literature.[76–78]

The feasibility of estimating the ^{241}Pu half-life value by applying the double ratio technique to QC data on CRMs 136, 137, 138, and 126 has been demonstrated.[79] The application of the double ratio technique to a smaller dataset than the one presented herein yielded a ^{241}Pu half-life value of 14.349 ± 0.023 years. In addition to the single ratio and double ratio techniques, the in-growth of the ^{241}Am daughter by IDMS has also been used to estimate the ^{241}Pu half-life value.[80]

For the TIMS instrumental data presented here, the double ratio shown in eqn[3] is used:

$$\frac{^{241}Pu/^{240}Pu}{^{240}Pu/^{239}Pu} = \frac{^{239}Pu \cdot {}^{240}Pu}{(^{240}Pu)^2}. \tag{3}$$

For the double ratio defined in eqn (3), the isotopic fractionation is given by using eqn (4):

$$\beta' = \sqrt{\left(\frac{m^{239}Pu \cdot m^{241}Pu}{(m^{240}Pu)^2}\right)} = 0.9999942 \tag{4}$$

Eqn (4) shows that for the $(^{239}Pu \cdot {}^{241}Pu)/(^{240}Pu)^2$ double ratio, deviations from unity are $100\times$ smaller than those for the single ratio, indicating negligible mass fractionation correction. Eqn (5) represents the relationship between the slope of the double ratio defined in eqn (3) and the decay constants of the three Pu isotopes:

$$\text{slope}_{\text{double ratio}} = \lambda_{241} + \lambda_{239} - 2\lambda_{240}. \tag{5}$$

Therefore, the ^{241}Pu decay constant can be expressed in terms of the slope of the double ratio and the decay constants of the ^{240}Pu and ^{239}Pu isotopes, as represented in eqn (6):

$$\lambda_{241} = \text{slope}_{\text{double ratio}} + 2\lambda_{240} - \lambda_{239}. \tag{6}$$

The half-life $\tau_{1/2}$ of ^{241}Pu can then be calculated from the decay constant using eqn (7):

$$\tau_{1/2}(^{241}Pu) = \frac{\ln(2)}{\lambda_{241}} \tag{7}$$

Half-life estimate from CRM 136

Fig. 20 shows a plot of the double ratio $vs.$ the decay time for CRM 136. For CRM 136, 352 measurements from 69 different
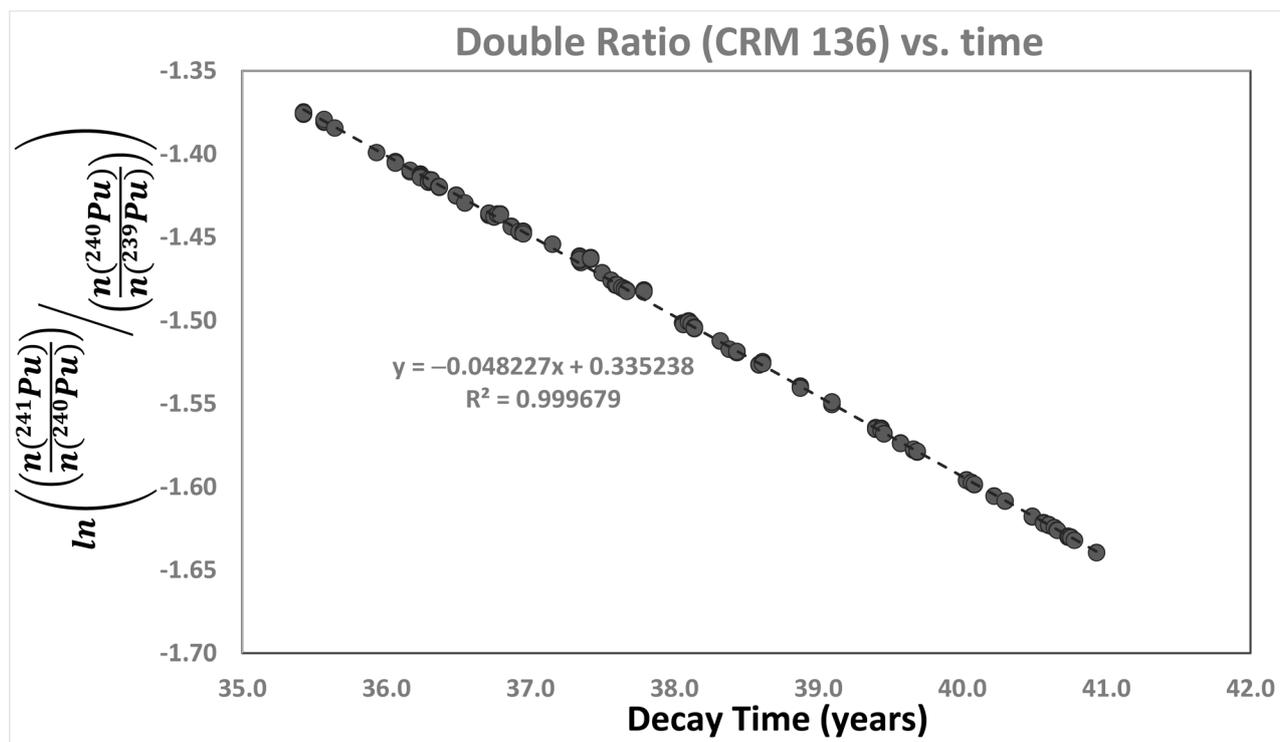

Fig. 20 Plot of the $(^{239}Pu \cdot {}^{241}Pu)/(^{240}Pu)^2$ ratio $vs.$ time for CRM 136. The slope of the linear regression line through the data and the correlation coefficient of the regression line are indicated.

separations performed over a period of 5.5 years are included in the double ratio plot. The slope of the regression line is 0.048227, which corresponds to a [241]Pu half-life value of 14.318 years.

For CRM 136, Fig. 21 shows a plot of the residuals from the line of best fit shown in Fig. 20. The data follow a normal distribution, as expected for a dataset with large degrees of freedom. Separations on two different days, marked by the dashed ellipsoidal, do not overlap the zero line within characteristic uncertainties of the measurements, indicating that small amounts of [241]Am remain in the Pu isotopic fraction measured. The Pu isotopic separations in the last 2.5 years included an additional rinsing step to completely remove the [241]Am from the Pu fraction measured for isotope ratios. The deviation from the zero line was significantly reduced (showing improvement by a factor of 2.2 in the standard deviation of the residuals) after the additional column rinse was introduced into the separation process.

Half-life estimate from CRM 137

Fig. 22 shows a plot of the double ratio *vs.* the decay time for CRM 137. For CRM 137, 205 measurements from 33 different separations performed over a period of 5.4 years are included in the half-life evaluation. The slope of the regression line is 0.048211, which corresponds to a [241]Pu half-life value of 14.323 years.

Fig. 23 shows a plot of residuals from the line of best fit in Fig. 22. As was the case for CRM 136, separations on a few days

do not overlap the zero line within the characteristic uncertainties of the data set, indicating that small amounts of [241]Am remain in the clean Pu isotopic fraction. An additional rinsing step in the Pu isotopic purification process was introduced for the separations in the last 2.5 years to completely remove the [241]Am from the Pu isotopic fraction. The deviation from the zero line was significantly reduced (showing improvement by a factor of 1.8 in the standard deviation of the residuals) after the additional column rinse was introduced into the separation process.

Half-life estimate from CRM 138

Fig. 24 shows a plot of the double ratio *vs.* the decay time for CRM 138. For CRM 138, 151 measurements from 22 different separations performed over a period of 5.4 years are included in the half-life evaluation. The slope of the regression line is 0.048171, which corresponds to a half-life value of 14.335 years for [241]Pu. Fig. 25 shows a plot of residuals from the line of best fit in Fig. 24. The deviation from the zero line was significantly reduced (showing improvement by a factor of 2.0 in the standard deviation of the residuals) after the additional column rinse was introduced into the separation process.

Half-life estimate from CRM 126-A

Fig. 26 shows a plot of the double ratio *vs.* the decay time for CRM 126-A. For CRM 126-A, 328 measurements from 72 different separations performed over a period of 5.5 years are included in the half-life evaluation. The slope of the regression
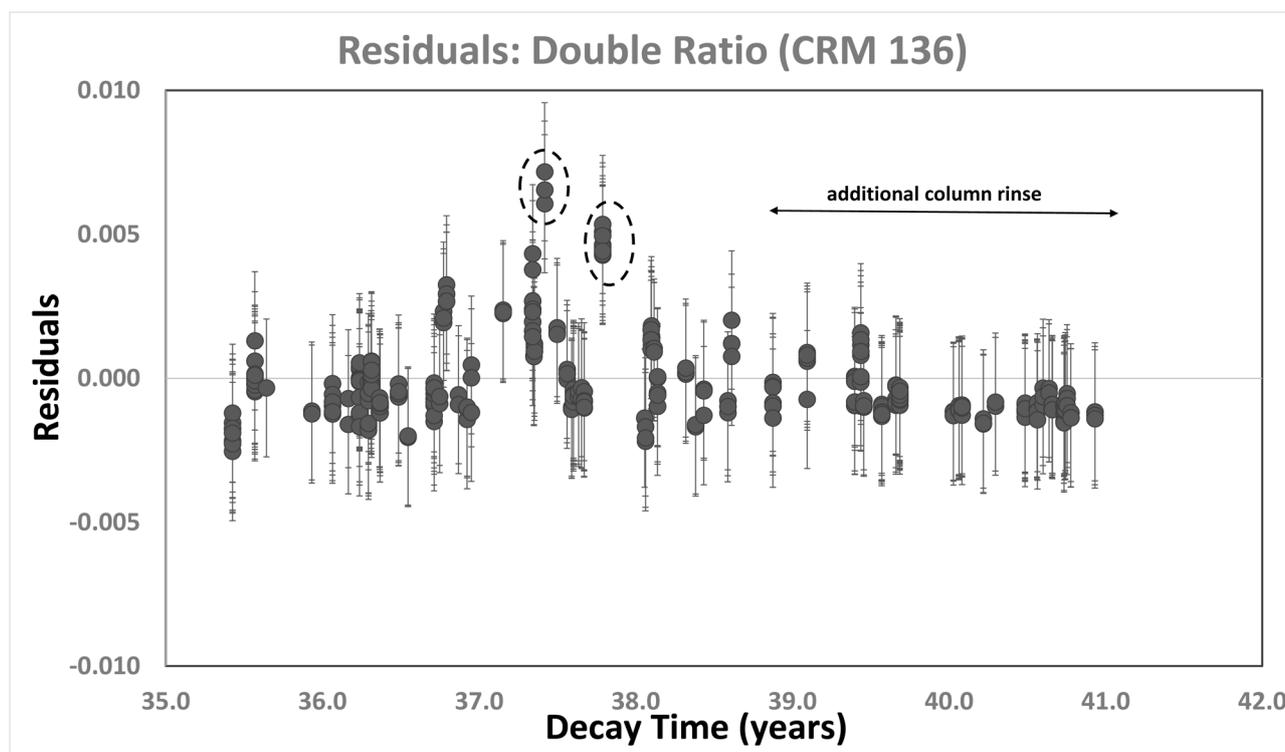

Fig. 21 Residuals of the individual data points from the line of best fit shown in Fig. 20 for CRM 136. A normal distribution around the "0.0" value (solid line) demonstrates the quality of the data.
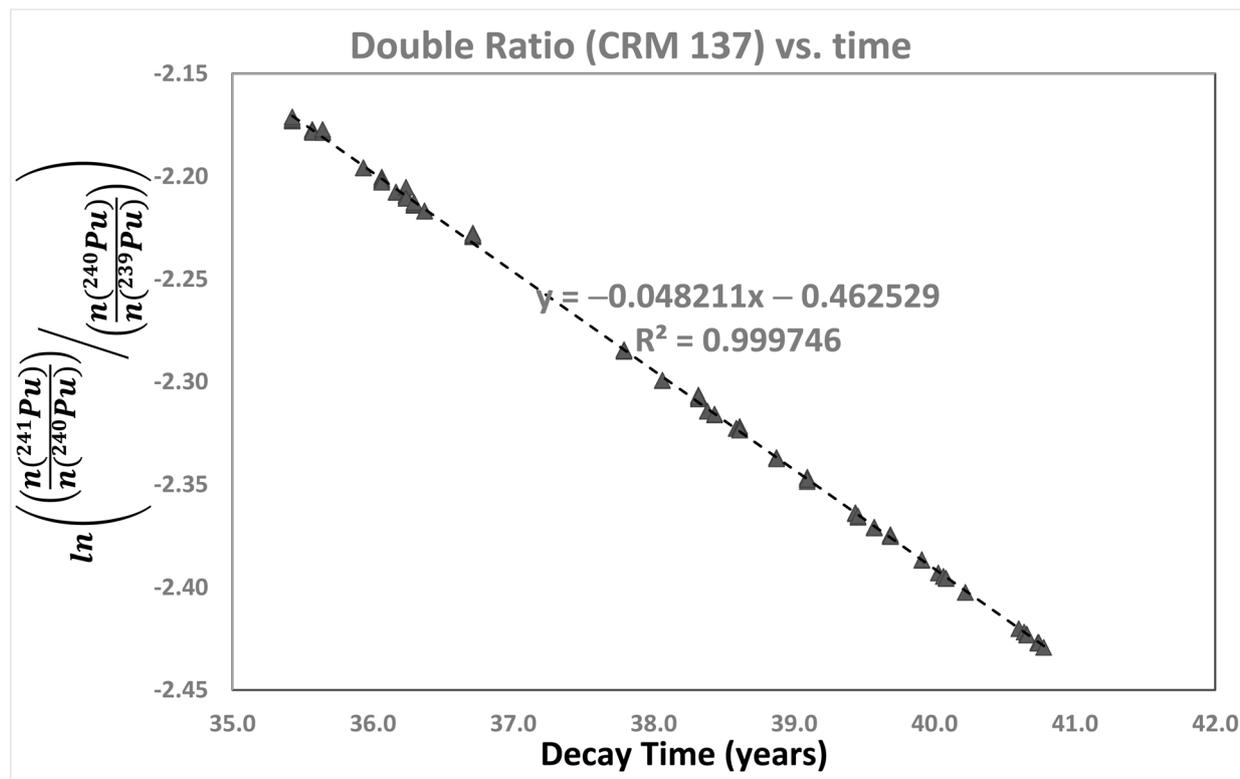
This journal is © The Royal Society of Chemistry 2025

J. Anal. At. Spectrom., 2025, **40**, 1879–1901 | **1895**

Fig. 22 Plot of the $(^{239}Pu \cdot ^{241}Pu)/(^{240}Pu)^2$ ratio *vs.* time for CRM 137. The slope of the linear regression line through the data and the correlation coefficient of the regression line are indicated.
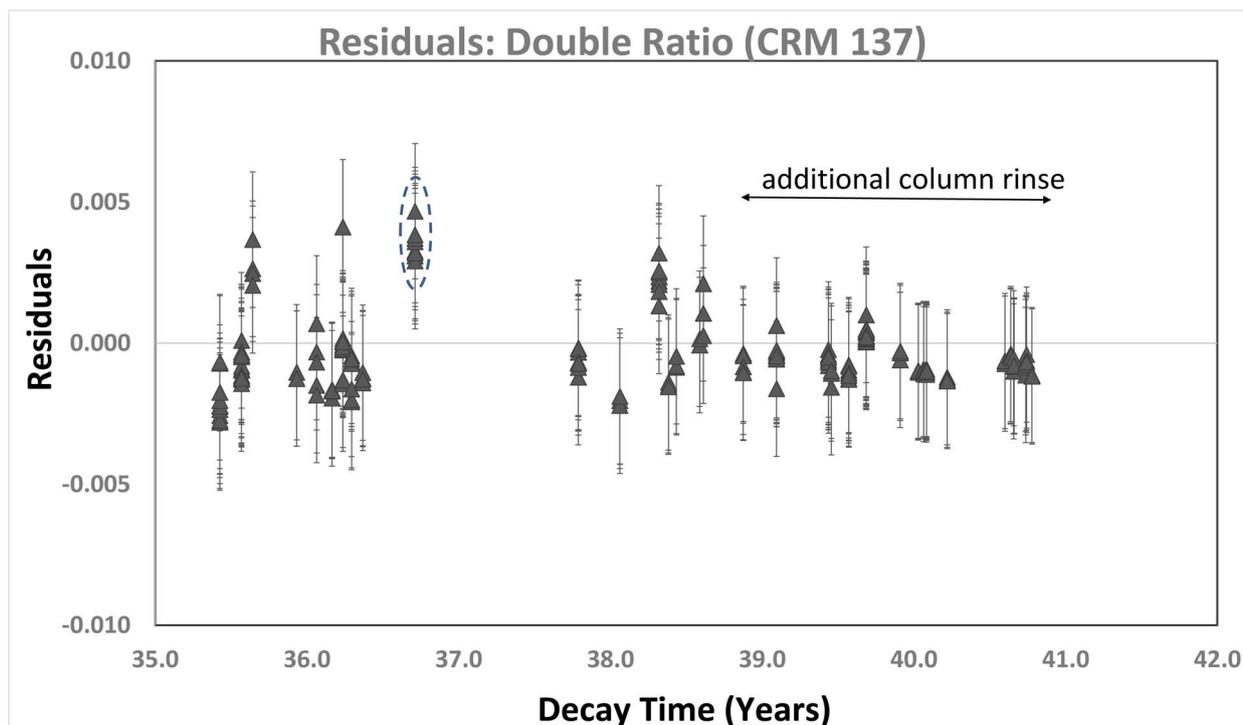

Fig. 23 Residuals of the individual data points from the line of best fit shown in Fig. 22 for CRM 137. A normal distribution around the "0.0" value (solid line) demonstrates the quality of the data.
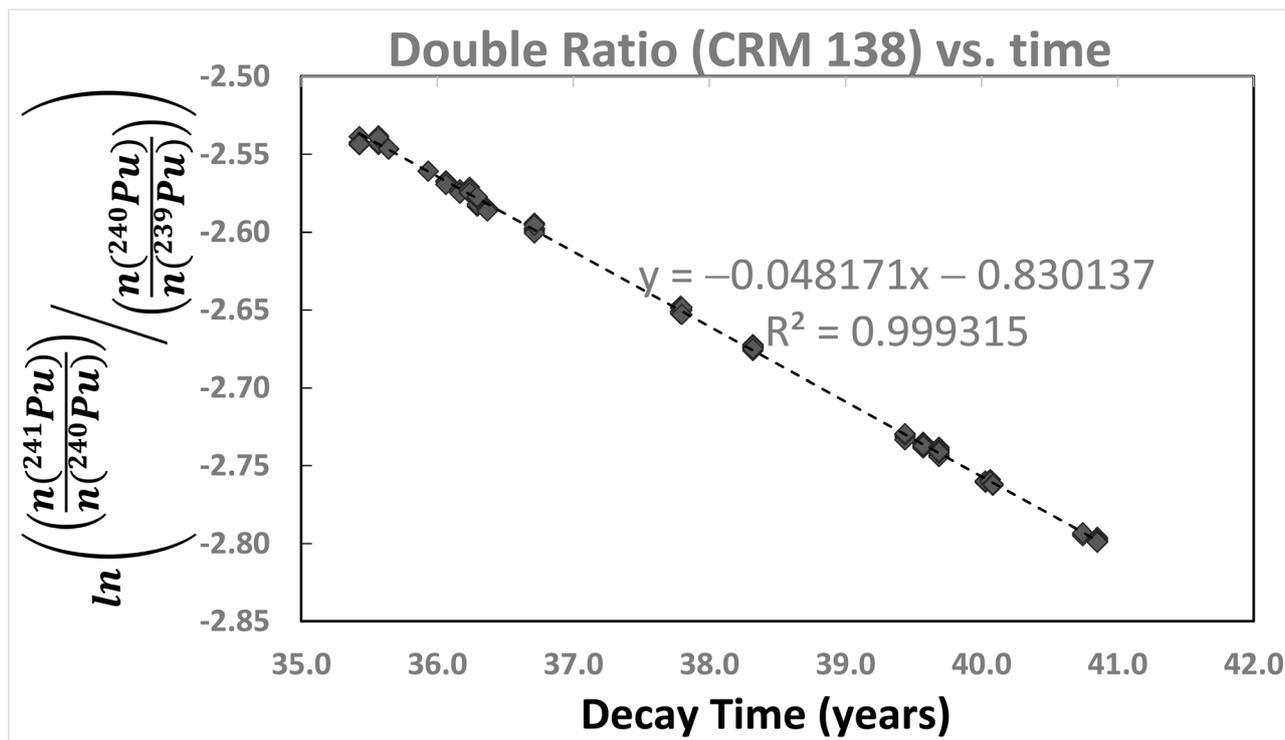
1896 | *J. Anal. At. Spectrom.*, 2025, **40**, 1879–1901

This journal is © The Royal Society of Chemistry 2025

Double Ratio (CRM 138) vs. time

$$\ln\left(\left(\frac{n(^{241}Pu)}{n(^{240}Pu)}\right)\Big/\left(\frac{n(^{240}Pu)}{n(^{239}Pu)}\right)\right)$$

$$y = -0.048171x - 0.830137$$
$$R^2 = 0.999315$$

Decay Time (years)

Fig. 24 Plot of the $(^{239}Pu \cdot {}^{241}Pu)/(^{240}Pu)^2$ ratio in CRM 138 *vs.* time. The slope of the linear regression line through the data and the correlation coefficient of the regression line are indicated.

Residuals: Double Ratio (CRM 138)
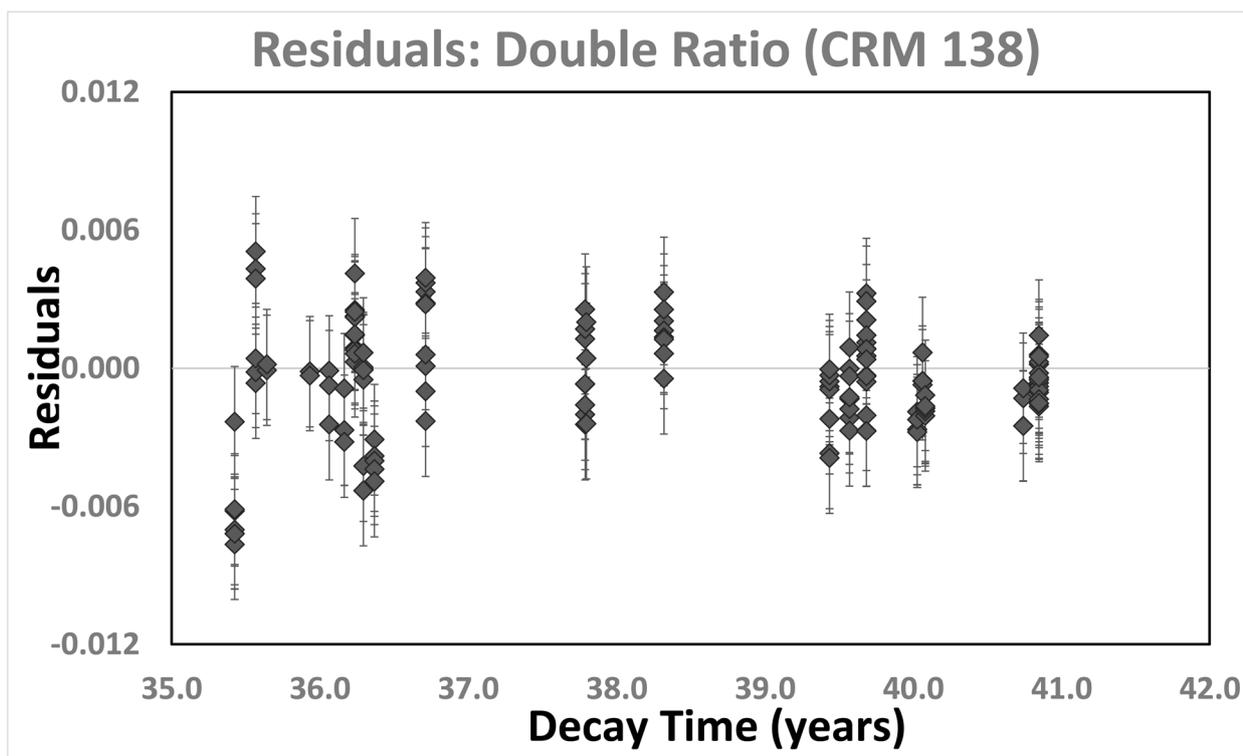
Residuals

Decay Time (years)

Fig. 25 Residuals of the individual data points from the line of best fit shown in Fig. 24 for CRM 138. A normal distribution around the "0.0" value (solid line) demonstrates the quality of the data.
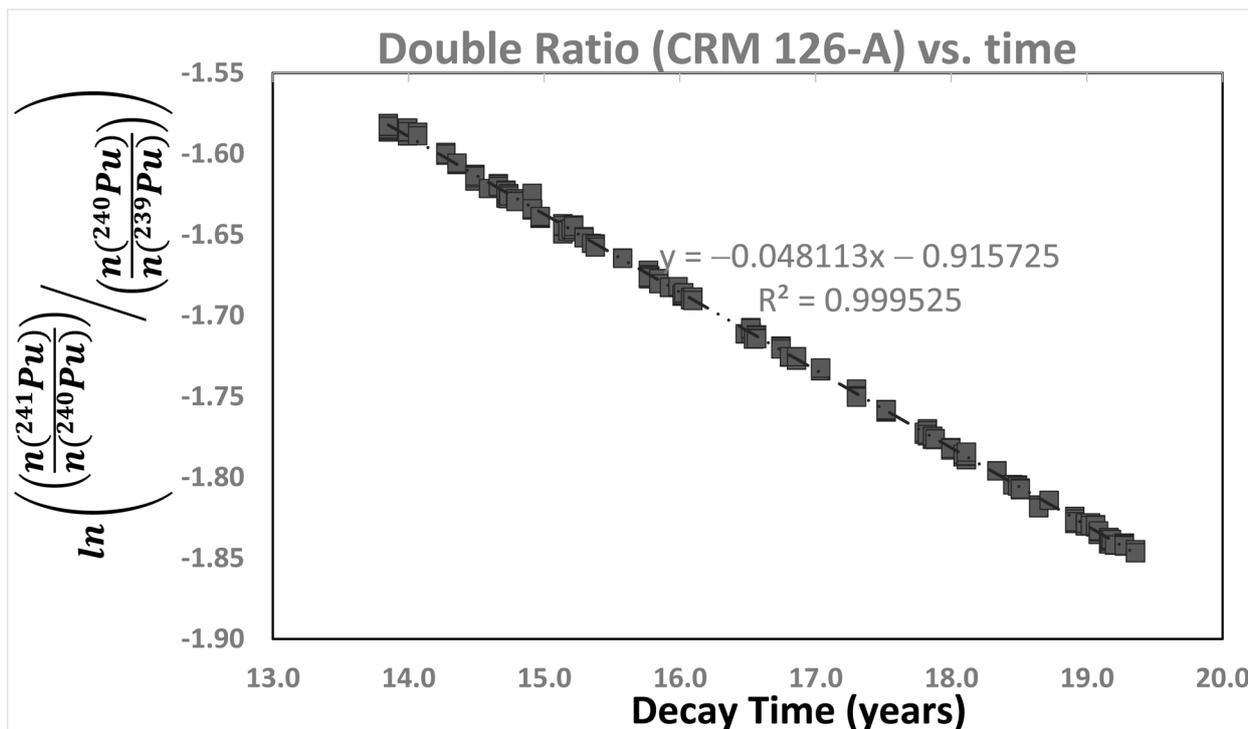
Fig. 26 Plot of the (^{239}Pu·^{241}Pu)/(^{240}Pu)^2 ratio in CRM 126-A *vs.* time. The slope of the linear regression line through the data and the correlation coefficient of the regression line are indicated.

line is 0.048113, which corresponds to a half-life value of 14.332 years for ^{241}Pu. Fig. 27 shows a plot of residuals from the line of best fit in Fig. 26. For the CRM 126-A dataset, the residuals follow a normal distribution around the zero line, as expected for a distribution with large degrees of freedom. The deviation from the zero line was significantly reduced (showing
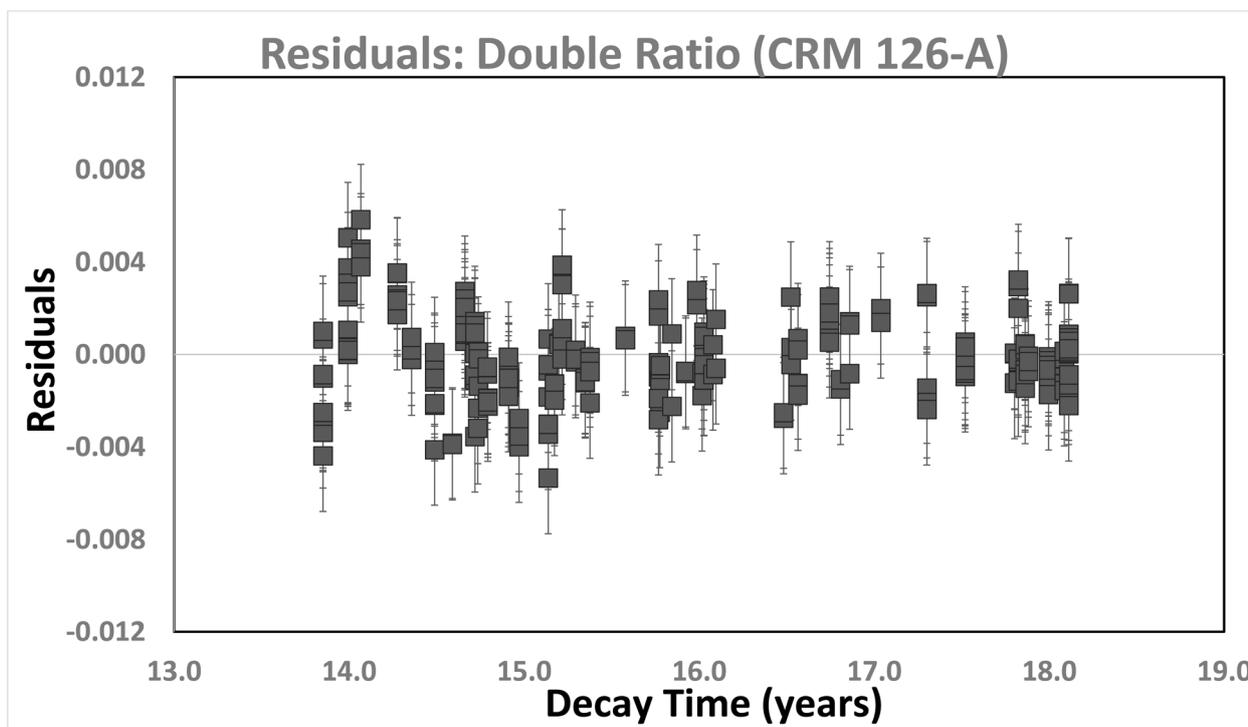

Fig. 27 Residuals of the individual data points from the line of best fit shown in Fig. 26 for CRM 126-A. A normal distribution around the "0.0" value (solid line) demonstrates the quality of the data.

1898 | *J. Anal. At. Spectrom.*, 2025, **40**, 1879–1901

This journal is © The Royal Society of Chemistry 2025

improvement by a factor of 1.4 in the standard deviation of the residuals) after the additional column rinse was introduced into the separation process.

Half-life estimate summary

The currently accepted half-life value for ^{241}Pu of 14.325 ± 0.024 years comes from Wellum et al.[78] This estimate is based on the application of the double ratio technique to TIMS data measured at the IRMM on a 93% purity ^{241}Pu material procured from the Oak Ridge National Laboratory (ORNL). An earlier estimate of 14.33 ± 0.02 years from De Bièvre et al.[77] (notably, the uncertainty quoted is 1σ) was also reported by the IRMM. In 2012, the IRMM performed additional measurements on the ORNL material that was used for the Wellum et al.[78] study. If the 2012 measurements are included in the Wellum et al.[78] published data, then a ^{241}Pu half-life value of 14.331 years is estimated (S. Richter, personal communication to K. Mathew on August 13, 2022). This new IRMM value shows excellent agreement with the value of 14.332 ± 0.017 years obtained in this investigation using the average slope value of the double ratio curves for the four different traceable CRMs from the NBL. The internal consistency of the half-life value from four independent traceable isotopic standards is a good demonstration of the fidelity of TIMS analytical data.

Conclusions

Conservative estimates for the $n(^{240}\text{Pu})/n(^{239}\text{Pu})$ major ratio uncertainties (expanded uncertainties expressed as the 95% confidence interval) in the range of approximately 0.024–0.030% have been obtained using long-term QC data for CRMs 136, 137, 138 and 126-A. These uncertainties represent state-of-practice uncertainties that can be achieved in Pu major isotope ratio measurements using modern multi-collector TIMS and ICP-MS instrumentation. For the $n(^{238}\text{Pu})/n(^{239}\text{Pu})$ minor isotope ratio, which is the ratio most affected by contributions from tailing, performing tailing corrections based on the observed biases on a per-turret basis improves the uncertainty of the ratio by a factor of 2 to 3. The HI-TE method has been demonstrated to further improve the uncertainty on this minor isotope ratio. A half-life of 14.332 ± 0.017 years was determined for the ^{241}Pu nuclide from high-fidelity measurements of traceable CRMs 136, 137, 138, and 126-A from the NBL. The ^{241}Pu half-life estimated herein from NBL CRMs shows excellent agreement with the currently accepted value using TIMS data from the IRMM. The data on four different Pu isotopic standards (two standards belonging to the high-burnup category and two other standards belonging to the low-burnup category) analyzed as part of routine measurements covering a performance period of approximately 5.5 years have been used for this half-life evaluation by the double ratio (or ratio of ratios) technique. The consistent value for the half-life of ^{241}Pu obtained from the four different Pu CRM standards demonstrates the high quality of the isotopic data obtained using TIMS instrumentation qualified to support the critical LANL mission of characterizing Pu materials.

Data availability

The data supporting this article have been included as part of the ESI.†

Conflicts of interest

There are no conflicts of interest to declare.

Acknowledgements

References

1 International Atomic Energy Agency, *Reference Data Series No. 1*, Vienna, Austria, 2020 edition.

2 S. Boulyga, S. Konegger-Kappel, S. Richter and L. Sangely, *J. Anal. At. Spectrom.*, 2015, **30**, 1469.

3 P. M. L. Hedberg, P. Peres, F. Fernandes and L. Renaud, *J. Anal. At. Spectrom.*, 2015, **30**, 2516.

4 E. Kuhn, D. Fischer and M. Ryjinksi, *Environmental sampling for IAEA safeguards: A five year review*, International Atomic Energy Agency (IAEA), Vienna, Austria, 2001, IAEA-SM-367.

5 IAEA, *Development and Implementation of Support Programme for Nuclear Verification 2018-1019*, International Atomic Energy Agency, Vienna, Austria, 2022, STR-386.

6 M. J. Kristo and S. J. Tumey, *Nucl. Instrum. Methods Phys. Res., Sect. B*, 2013, **294**, 656.

7 K. Mayer, M. Wallenius and T. Fanghänel, *J. Alloys Compd.*, 2007, **444–445**, 50.

8 G. Nikolaou and S. R. Biegalski, *J. Radioanal. Nucl. Chem.*, 2019, **322**, 513.

9 L. Tandon, K. Kuhn, P. Martinez, J. Banar, L. Walker, et al., *J. Radioanal. Nucl. Chem.*, 2009, **282**, 573.

10 Z. Varga, R. Katona, Z. Stefánka, M. Wallenius, K. Mayer and A. Nicholl, *Talanta*, 2010, **80**, 1744.

11 Z. Varga, K. Mayer, C. E. Bonamici, A. Hubert, I. Hutcheon, et al., *Appl. Radiat. Isot.*, 2015, **102**, 81.

This journal is © The Royal Society of Chemistry 2025

J. Anal. At. Spectrom., 2025, **40**, 1879–1901 | **1899**

12 Z. Varga, M. Wallenius and K. Mayer, *J. Anal. At. Spectrom.*, 2010, **25**, 1958.

13 M. Wallenius and K. Mayer, *Fresenius. J. Anal. Chem.*, 2000, **366**, 234.

14 M. Wallenius, K. Mayer and I. Ray, *Forensic Sci. Int.*, 2006, **156**, 55.

15 R. P. Keegan and R. J. Gehrke, *Appl. Radiat. Isot.*, 2003, **59**, 137.

16 M. Wallenius, P. Peerani and L. Koch, *J. Radioanal. Nucl. Chem.*, 2000, **246**, 317.

17 M. Sturm, S. Richter, Y. Aregbe, R. Wellum, S. Mialle, *et al.*, *J. Radioanal. Nucl. Chem.*, 2014, **302**, 399.

18 M. Wallenius, K. Lützenkirchen, K. Mayer, I. Ray, L. A. de las Heras, *et al.*, *J. Alloys Compd.*, 2007, **57**, 444–445.

19 E. Keegan, M. Wallenius, K. Mayer, Z. Varga and G. Rasmussen, *Appl. Geochem.*, 2012, **27**, 1600.

20 J. H. Rim, K. J. Kuhn, L. Tandon, N. Xu, D. R. Porterfield, *et al.*, *Forensic Sci. Int.*, 2017, **273**, e1.

21 L. Tandon, E. Hastings, J. Banar, J. Barnes, D. Beddingfield, *et al.*, *J. Radioanal. Nucl. Chem.*, 2008, **276**, 467.

22 K. Mayer, M. Wallenius and Z. Varga, *Chem. Rev.*, 2013, **113**, 884.

23 A. Glaser, *Nucl. Sci. Eng.*, 2009, **163**, 26.

24 E. Keegan, M. J. Kristo, M. Colela, M. Robel, R. Williams, *et al.*, *Forensic Sci. Int.*, 2014, **240**, 111.

25 M. J. Kristo, E. Keegan, M. Colela, R. Williams, R. Lindavall, *et al.*, *Radiochim. Acta*, 2015, **103**(7), 487.

26 S. Niemeyer and I. Hutcheon, in *Advances in Destructive and Non-Destructive Analysis for Environmental Monitoring and Nuclear Forensics, Proceedings of International Conference, Karlsruhe*, Vienna, 2002, Int. At. Energy Agency.

27 S. Baude, B. Chartier, D. Kimmel, F. Marriotte and D. Masse *et al.*, in *Illicit Nuclear Trafficking; Collective Experience and the way Forward. Proceedings of International Conference*, Edinburgh, 2007, 363, Vienna Int. At. Energy Agency.

28 International Atomic Energy Agency, 2014, *IAEA Incident and Trafficking Database (ITDB): Fact Sheet*, retrieved from http://www-ns.iaea.org/downloads/security/itdb-fact-sheet.pdf.

29 G. Tamborini and M. Betti, *Mikrochim. Acta*, 2000, **132**, 411.

30 G. Tamborini, M. Wallenius, O. Bildstein, L. Pajo and M. Betti, *Mikrochim. Acta*, 2002, **139**, 185.

31 M. Wallenius, G. Tamborini and L. Koch, *Radiochim. Acta*, 2001, **89**, 55.

32 M. Kraiem, S. Richter, H. Kühn, E. A. Stefaniak, G. Kerckhove, J. Truyens and Y. Aregbe, *Anal. Chem.*, 2011, **83**, 3011.

33 T. Shinonaga, F. Esaka, M. Magara, D. Klose and D. Donohue, *Spectrochim. Acta, Part B*, 2008, **63**, 1324.

34 Strumińska-Parulska, *J. Radioanal. Nucl. Chem.*, 2013, **298**, 593.

35 G. R. Eppich, R. W. Williams, A. M. Gaffney and K. C. Schorzman, *J. Anal. At. Spectrom.*, 2013, **28**, 666.

36 A. M. Gaffney, A. Hubert, W. S. Kinman, M. Magara and A. Okubo, *J. Radioanal. Nucl. Chem.*, 2015, **307**, 2055.

37 T. M. Kayzar and R. W. Williams, *J. Radioanal. Nucl. Chem.*, 2016, **307**(3), 2061.

38 A. Morgenstern, C. Apostolidis and K. Mayer, *Anal. Chem.*, 2002, **74**, 5513.

39 S. Richter, A. Alonso, W. De Bolle, R. Wellum and P. D. P. Taylor, *Int. J. Mass Spectrom.*, 1999, **193**, 9.

40 K. J. Spencer, L. Tandon, D. Gallimore, N. Xu and K. Kuhn, *J. Radioanal. Nucl. Chem.*, 2009, **282**, 549.

41 M. Wallenius, A. Morgenstern, C. Apostolidis and K. Mayer, *Anal. Bioanal. Chem.*, 2002, **374**, 379.

42 R. W. Williams and A. M. Gaffney, *Proc. Radiochim. Acta*, 2011, **1**, 31.

43 K. Mathew, T. Kayzar-Boggs, Z. Varga, A. Gaffney, J. Denton, *et al.*, *Anal. Chem.*, 2019, **91**(18), 11643.

44 F. E. Stanley, *J. Anal. At. Spectrom.*, 2012, **27**, 1821.

45 F. E. Stanley, A. M. Stalcup and H. B. Spitz, *J. Radioanal. Nucl. Chem.*, 2013, **295**, 1385.

46 K. J. Mathew, C. Ottenfeld and N. Butterfield, *J. Radioanal. Nucl. Chem.*, 2022, **331**, 4881.

47 S. C. Metzger, B. W. Ticknor, K. T. Rogers, D. A. Bostick, E. H. McBay and C. R. Hexel, *Anal. Chem.*, 2018, **90**(15), 9441.

48 S. Richter, C. Hennessy, J. Truyens, U. Jacobsson, C. Venchiarutti, R. Bujak and Y. Aregbe, *J. Radioanal. Nucl. Chem.*, 2024, **333**(2), 825.

49 P. Mason and U. Narayanan, *New Brunswick Laboratory Report*, NBL-RM-2010-Pu-History, 2010.

50 E. L. Garner, L. A. Machlan and W. R. Shields, NBS publication 260-27, 1971.

51 K. J. Mathew, F. E. Stanley, M. R. Thomas, K. J. Spencer, L. P. Colletti and L. Tandon, *Anal. Methods*, 2016, **8**, 7289.

52 S. Bürger, S. D. Balsley, S. Baumann, J. Berger, S. F. Boulyga, J. A. Cunningham, S. Kappel, A. Koepf and J. Poths, *Int. J. Mass Spectrom.*, 2012, **311**, 40.

53 S. Bürger, R. M. Essex, K. J. Mathew, S. Richter and R. B. Thomas, *Int. J. Mass Spectrom.*, 2010, **294**, 65.

54 S. Richter, J. Truyens, C. Venchiarutti, Y. Aregbe, R. Middendorp, *et al.*, *J. Radioanal. Nucl. Chem.*, 2023, **332**, 2809.

55 R. Middendorp, M. Dürr, A. Knott, F. Pointurier, D. F. Sanchez, V. Samson and D. Grolimund, *Anal. Chem.*, 2017, **89**, 4721.

56 R. M. Abernathey, G. M. Matlack and J. E. Rein, in *Analytical Methods in the Nuclear Fuel Cycle*, International Atomic Energy Agency, Vienna, Austria, 1972, p. 513.

57 E. P. Horwitz, R. Chiarizia, M. L. Dietz, H. Diamond and D. M. Nelson, *Anal. Chim. Acta*, 1993, **281**, 361.

58 Standard Test Method for Determination of Uranium or Plutonium or Americium Isotopic Composition or Concentration by the Total Evaporation Method Using a Thermal Ionization Mass Spectrometer, C1672-23.

59 M. Romkowski, S. Franzini and L. Koch, *Proceedings of the 8th Annual ESARDA Symposium*, London, 1987, pp. 12–14.

60 R. Fielder, *Int. J. Mass Spectrom.*, 1995, **146/147**, 91.

61 E. L. Callis and R. M. Abernathy, *Int. J. Mass Spectrom.*, 1991, **103**, 93.

62 K. J. Mathew, G. O'Connor, A. Hasozbek and M. Kraiem, *J. Anal. At. Spectrom.*, 2013, **28**, 866.

1900 | *J. Anal. At. Spectrom.*, 2025, **40**, 1879–1901

This journal is © The Royal Society of Chemistry 2025

63 K. J. Mathew, *Plutonium Handbook, 2nd Edition*, ed. D. L. Clark, D. A. Geeson and R. J. Hanrahan, American Nuclear Society, 2019, vol. 6, p. 3392.

64 K. J. Mathew, C. Ottenfeld, R. Keller and A. Slemmons, *J. Radioanal. Nucl. Chem.*, 2018, **318**(1), 395.

65 R. Jakopic, A. Fankhauser, Y. Aregbe, M. Crozet and C. Maillard *et al.*, *EUR 28748 EN*, Publications Office of the European Union, Luxembourg, 2017, p. JRC107840, ISBN 978-92-79-72281-3, DOI: **10.2760/40283**.

66 K. J. Mathew, C. F. Ottenfeld, R. C. Keller, K. J. Kuhn and J. B. Fulwyler, *Int. J. Mass Spectrom.*, 2020, **458**, 116430.

67 S. Richter, H. Kühn, Y. Aregbe, M. Hedberg, J. Horta-Domenech, *et al.*, *J. Anal. At. Spectrom.*, 2011, **26**, 550.

68 S. Richter and S. A. Goldberg, *Int. J. Mass Spectrom.*, 2003, **229**, 181.

69 K. J. Mathew, R. M. Essex, C. Gradle and U. Narayanan, *J. Radioanal. Nucl. Chem.*, 2015, **305**(1), 277.

70 T. E. Sampson, in *Passive Nondestructive Assay of Nuclear Materials*, US Nuclear Regulatory Commission, NUREG/CR-5550, 1991, ch. 8, LA-UR-90-732.

71 *International Target Values 2020 for Measurement Uncertainties in Safeguarding Nuclear Materials*, International Atomic Energy Agency, Vienna, Austria, STR-368 (R1.1).

72 K. J. Mathew and C. Ottenfeld, *Development, Qualification, and Performance of a High Intensity Total Evaporation Method for Characterization of Plutonium Isotopic Certified Reference Materials*, Fall Meeting, AGU, Chicago, 2022.

73 S. F. Marsh, R. M. Abernathey, R. J. Beckman and J. E. Rein, *Int. J. Appl. Radiat. Isot.*, 1980, **31**, 629.

74 E. L. Garner and L. A. Machlan, in *Measurement Technology for Safeguards and Materials Control, Proc. American Nuclear Society Topical Meeting*, Kiwah Island, South Carolina, National Bureau of Standards Publication, 1979, vol. 582, p. 34.

75 R. K. Zeigler and Y. Ferris, *J. Inorg. Nucl. Chem.*, 1973, **35**, 3417.

76 M. J. Cabell, *J. Inorg. Nucl. Chem.*, 1968, **30**, 2583–2589.

77 P. De Bièvre, M. Gallet and R. Werz, *Int. J. Mass Spectrom. Ion Phys.*, 1983, **51**, 111.

78 R. Wellum, A. Verbruggen and R. Kessel, *J. Anal. At. Spectrom.*, 2009, **24**, 801.

79 K. J. Mathew, C. Ottenfeld and N. Butterfield, *Weapons Eng. Science Journal*, 2022, LA-CP-24-10643, Los Alamos National Laboratory, Los Alamos, New Mexico, USA, 2024.

80 S. K. Aggarwal and H. C. Jain, *Phys. Rev. C*, 1980, **21**, 2033.

This journal is © The Royal Society of Chemistry 2025

J. Anal. At. Spectrom., 2025, **40**, 1879–1901 | **1901**